DEVELOPMENT OF NOVEL GENETIC CIRCUITS FOR THE DETECTION OF DISEASE BIOMARKERS

A Dissertation

Presented to the Faculty of the Graduate School

of Cornell University

In Partial Fulfillment of the Requirements for the Degree of

Doctor of Philosophy

by

Thomas Christopher Aurand

May 2016

DEVELOPMENT OF NOVEL GENETIC CIRCUITS FOR THE DETECTION OF DISEASE BIOMARKERS

Thomas Christopher Aurand, Ph. D.

Cornell University 2016

The US Centers for Disease Control and Prevention (CDC) estimates chronic diseases account for 86% of the annual health care costs in the US. Monitoring and intervention of chronic diseases such as cardiovascular disease, diabetes, and arthritis, are required to decelerate their progression. Some markers of these diseases are secreted into the intestine, providing an alternative monitoring approach. The development of bacteria based environmental sensors, or bioreporters using synthetic biology techniques provides a novel approach to monitor disease biomarkers.

In the studies presented here, we developed two novel bioreporter systems using genetic circuits to monitor disease biomarkers. We identified the peptide fragments of the outer membrane protein, OprF of *Pseudomonas aeruginosa* which bind interferon-γ (IFN-γ) and interact with tumor necrosis factor-α (TNF-α). We engineered sensors for IFN-γ and TNF-α as fusion proteins of OmpA/OprF, expressed in *Escherichia coli*. The phage shock protein A, *pspA* promoter was used for the first time to transduce the interaction of the markers with the OmpA/OprF sensor into a quantifiable signal, measured as β-galactosidase activity. This novel detection system for IFN-γ and TNF-α was capable of detecting these inflammatory markers. Subsequently, the detection systems were tested in an *in vitro* model of intestinal barrier dysfunction. Direct application of the bioreporter systems to the intestinal

"lumen" portion of the model demonstrated strong detection of the cytokines which diffused through the permeable barrier, showing the promise for the potential advancement to use *in vivo* models. The threshold detection concertation for the bioreporter systems was in the active range observed in stool samples of patients with Inflammatory Bowel Disease.

Secondly, we developed a detection system for elevated concentrations of uric acid, which are implicated in gout, a form of arthritis. We used the transcriptional regulator, PucR of the purine catabolism pathway of *Bacillus subtilis* to develop a synthetic promoter responsive to uric acid, driving the production of GFP. With this novel system we could differentiate between healthy and hyperuricemic concentrations of uric acid observed in the gut. The sensor systems we developed in these studies provide an essential contribution to the development of future diagnostic systems and active therapeutics.

BIOGRAPHICAL SKETCH

Chris Aurand is originally from Orchard Park, NY. Chris moved to Canada after finishing high school at Orchard Park High School. Chris attended the University of Guelph (Ontario, Canada) to pursue a Bachelor's degree in Food Science. During Chris's time at Guelph, he had the opportunity to conduct research in the field of lipid crystallization, under the supervision of Dr. Alejandro Marangoni and colleagues. In 2006 Chris participated in the Cornell Food Science Summer Scholar program and conducted research with Dr. Syed Rizvi. In the summer of 2007 Chris had a summer internship at the National Space Biomedical Research Institute, (Houston, Texas) where he worked in the Space Food Systems Laboratory at the Johnson Space Center. In 2007 Chris attended the University of Massachusetts Amherst to conduct research in the field of emulsion delivery systems for antimicrobial compounds under the supervision of Dr. Jochen Weiss. During his time at Amherst, Chris took leadership roles in the Food Science club and IFT Product Development Competitions. Chris also took a course taught by Dr. Susan Roberts which inspired him to pursue research in the field of synthetic biology which he plans to apply to the discipline of food science. In 2009, Chris joined the Department of Food Science at Cornell University to pursue a Ph.D. in the Metabolic and Signal Engineering Laboratory under the supervision of Dr. John March. Chris has mentored multiple undergraduate and high school students in the laboratory and classroom settings. Chris was a team leader for the Dairy Research Institute New Product Development Competition in which his teams' product was selected as a finalist. Chris has also been involved with the Graduate and Professional Student Assembly as

a voting representative of the Biological Sciences. In his free time, Chris enjoys traveling, car restoration, brewing, and skiing.

This dissertation is dedicated to my grandfather, Professor Leonard W. Aurand for his encouragement and guidance in pursuing a career in science.

ACKNOWLEDGMENTS

I would like to express my deepest gratitude to Dr. John March for the opportunity to work in his research group, and for all his support and mentorship throughout my degree. I would also like to thank my committee members, Dr. Ruth Ley and Dr. Cynthia Reinhart-King, for their support. Thank you to all the current and former members of the March Lab, for all the support in the lab and being there to rely on. Thank you, Faping, Houchun, Jiajie, Yih Lin, Hongfei, Owen, Cait, Caitlin, Mikkel, Gözde and Julie and my undergraduate student, Chris for all the contributions you have made to making my time at Cornell enjoyable. In particular, I would like to thank Faping and Matt for all the help and guidance they provided in learning new molecular biology techniques.

I would also like to thank my friends and family for the continued support throughout my time at Cornell. My parents, Tom and Kay, for their guidance and advice in the development of my career and life, I cannot thank you enough. I would like to thank my grandfather, Leonard Aurand for always asking the hard scientific questions about my research and for inspiring me at a young age to pursue my passion in the sciences. Lastly, I would like to thank my girlfriend Kitiya for being there for me throughout this process.

TABLE OF CONTENTS

LIST OF FIGURES

LIST OF TABLES

CHAPTER ONE

Introduction

The research presented in this dissertation was designed to contribute to two major goals; (1) develop a whole cell bioreporter for the detection of the inflammatory cytokines IFN-γ, TNF-α and test the detection capacity of the whole cell bioreporter in an *in vitro* model of a dysfunctional intestinal barrier; and (2) develop a whole cell biosensor for the detection of uric acid at estimated concentrations present in the intestinal lumen of hyperuricemic individuals. This introductory chapter presents information relevant to achieving these goals.

Chronic or non-communicable diseases are life-long diseases that require monitoring and management in order to maintain an acceptable quality of life. The US Centers for Disease Control and Prevention (CDC) estimates that chronic diseases account for 70% of the yearly deaths in the US and result in 86% of the annual health care costs (Gerteis et al. 2014). Further, the World Health Organization projects the occurrence of chronic diseases will increase in the coming decades (Mendis. et al. 2014). The progression of chronic diseases such as cardiovascular disease, diabetes, arthritis and weak or failing kidneys can be decelerated by lifestyle changes and regular monitoring of disease progression (Ancker et al. 2015; Ward et al. 2014). Currently, the standard method to monitor and diagnose chronic disease progression is to visit a physician and have blood tests or other diagnostic tests performed. However, visiting a physician can be time consuming and there is interest in the development of methods to monitor disease biomarkers by less invasive and convenient means.

An alternative monitoring method would be to detect disease contributors in

the intestinal tract, for example, biomarkers of chronic inflammation, a large component to the progression of chronic diseases (Pearson et al. 2003; Bischoff et al. 2014; Arrieta et al. 2006). Compounds enter the intestinal lumen by secretion or diffuse through the intestinal barrier, permitting an opportunity to detect concentration changes or the presence of disease biomarkers. For example, detection of elevated levels of uric acid for hyperuricemia (Hosomi et al. 2012), or intestinal alkaline phosphatase for metabolic syndrome (Lallès 2015) would permit a means to determine changes in disease progression. On the other hand, biomarkers permeate into the intestinal lumen during chronic inflammation contributing to the leakiness of the intestinal barrier, such as calprotectin in inflammatory bowel disease (IBD), interferon-γ (IFN-γ) in IBD (Lainscak et al. 2009) and gastrointestinal infection (Enocksson et al. 2004) or tumor necrosis factor-α (TNF-α) in IBD (Braegger et al. 1992). The appearance or change of disease biomarkers in the intestinal lumen provides a new, non-invasive approach to monitor for disease development and progression.

The Intestine

The principal function of the small and large intestine is the absorption of nutrients and excretion of compounds. The intestines provide this function while acting as a barrier against the external environment preventing microorganisms and antigens from crossing into the body. Intestinal epithelial cells (IECs) make up the majority of this barrier and interact with the luminal contents of the gut including the microbiota. The IECs are the main contributor to transport of nutrients across the barrier by two transport pathways, transcellular and paracellular pathways (Rescigno

2011). The transcellular pathway involves the active transport of molecules through IECS, in which the molecule crosses the apical and basolateral membrane of the cell (Robinson et al. 2015) The paracellular pathway is where molecules pass between a selectively permeable barrier, formed between IECs by tight junctions which are dynamic, multifunctional complexes of proteins (Ulluwishewa et al. 2011). Permeability of tight junctions is regulated by physiological and external stimuli such as commensal bacteria (Madsen et al. 2001), and food components (gliadin from wheat) (Drago et al. 2006). Tight junctions govern paracellular transport of molecules by the formation of two types of pores; restrictive pores which permit diffusion of water, ions, and other small molecules, and non-restrictive pores that allow large, hydrophilic molecules to pass (dextran and graded polyethylene polymers) (Watson et al. 2001). Further, paracellular pores permit the excretion of compounds into the intestinal tract such as uric acid (Ogura et al. 2012). The intestine excretes approximately one third of the daily turnover of uric acid (Sorensen 1965). The excretion rate of uric acid by means of the intestinal pathway is correlated to high serum levels of uric acid, which have been implicated in contributing to gout (Kutzing & Firestein 2008), cardiovascular disease (Progress et al. 2008), and diabetes (Bhole et al. 2015). The excretion of uric acid into the gastrointestinal tract would therefore permit a sensor to be developed to monitor uric acid concentrations in the gut.

However, under conditions of inflammation the intestinal barrier becomes "leaky", permitting antigens and microbes to cross the barrier and immunoregulators to be released into the intestinal lumen (Al-Sadi et al. 2009). The leakiness of the intestinal barrier is governed by modification of the tight junctions in response to

inflammatory cytokines, changing the selectivity of the nonrestrictive pores of the paracellular pathway (Watson et al. 2005). The intestinal barrier becomes leaky during inflammation based diseases such as inflammatory bowel disease, (IBD) (Crohn's disease and ulcerative colitis), irritable bowel disease (IBS), and bacterial infection (Al-Sadi et al. 2009). During a healthy immune response, the immune system would eliminate the causative agent and subsequently, resolve. However, in situations of chronic inflammation such as IBD, the upregulated immune response does not resolve once the agonist has been removed (Papadakis & Targan 2000). Increased concentrations of pro-inflammatory cytokines; interferon-γ (IFN-γ), tumor necrosis factor-α (TNF-α), interleukin-1β (IL-1β) and IL-12 present in the submucosa during chronic inflammation lead to further increases in intestinal epithelial permeability allowing for the inflammatory cycle to persist (Al-Sadi et al. 2009).

The pro-inflammatory cytokines IFN-γ and TNF-α have been implicated in the pathogenesis of IBD (MacDonald et al. 1990). IFN-γ and TNF-α have been shown to increase intestinal permeability independently and synergistically (Madara & Stafford 1989; Ma et al. 2004; Fish et al. 1999). Watson *et al* (2005) showed that IFN-γ induced a selective increase in paracellular permeability for larger molecules (7.4 - 23 Å). The selective increase in permeability of larger molecules to translocate across the epithelial barrier may also permit the release of inflammatory cytokines and other disease biomarkers into the intestinal lumen. Measuring the presence of abnormal concentrations of cytokines in the lumen could be used for detection of the onset and relapse of IBD. A previous study by Braegger *et al* (1992) demonstrated that TNF-α could be detected in the stool of patients with Crohn's disease and

ulcerative colitis at concentrations of 57.1 pM and a range of 15.9-343.8 pM respectively, whereas controls had an average TNF-α concentration of 3.3 pM. However, IFN-γ concentrations have not been reported in stool samples of IBD patients, which may be a result of the state of disease progression (Bisping et al. 2001; Ito et al. 2006; Neurath 2014). Spencer *et al* (2002) conducted a longitudinal study of colitis in mice, monitoring inflammation progression and showed that IFN-γ production increases during early stages of colitis and dissipated at late stages, whereas, TNF-α production was constant throughout the disease. This suggests there would be a benefit for a more localized and rapid detection system. A bacterial based bioreporter could fill this need, providing a method of detection that is noninvasive and situated to localized detection by means of oral administration (Carty et al. 2000; Aurand et al. 2012).

Environmental detection

The intestinal barrier dynamically interacts with the environment, selectively permitting the exchange of compounds across this barrier. Monitoring changes in this exchange or initial detection of compounds establishes a new means to determine the health of a host. The microbiota has evolved alongside the host to interact with the intestinal barrier in both a beneficial or detrimental fashion. The capacity of bacteria to monitor environmental factors such as pH, osmolarity, small molecules and ligands is essential for their survival. Determination of environmental changes allows bacteria to adapt and survive in the current environment. For example, the food-borne pathogen enterohemorrhagic *E. coli* (EHEC) O157:H7, senses host-produced adrenaline, noradrenaline or gastrointestinal microbial flora derived quorum sensing

signal, autoinducer-3 (AI-3) alerting the pathogen that it is within a host and activating EHEC's virulence genes of the locus of enterocyte effacement (LEE), pathogenicity island (Sperandio et al. 2003; Clarke et al. 2006). Activation of LEE induces expression of genes involved in acid tolerance, attachment and effacing of the colonic epithelial barrier giving EHEC a distinct advantage to colonize the intestine and outcompete protective commensal bacteria (Luck et al. 2005; Nguyen & Sperandio 2012). The capacity of bacteria to determine environmental factors and activate a network of genetic responses is central to the development of novel circuits for the discipline of synthetic biology.

The fundamental concept of synthetic biology is the understanding that bacteria use networks of genes to respond to the environment, composed of individual genetic components or cassettes which could be rearranged in a rational manner for the development of novel systems (Jacob & Monod 1961). The development of molecular cloning techniques, PCR and genetic sequencing allowed for a better understanding of these genetic systems and how the modular components of these systems interacted (Cameron et al. 2014). This understanding that components of these genetic networks were modular and could rationally reorganized to form new genetic networks for biotechnology and therapeutic applications led to the development of the field of synthetic biology (Benner 2003).

The similarity of genetic networks to electronic control circuits gave rise to the use of engineering concepts of modularity and a need to standardize individual components for the reprograming of cellular behavior in a predictable manner (Ausländer & Fussenegger 2013). The genetic networks used by bacteria to sense and

respond to environmental factors can be broken down into individual components; of which a receptor interacts with the extracellular signal (signal input), signal transduction (signal processor), which activates a reporter gene (output). The individual components of multiple networks can be reorganized or modified to develop novel circuits to process multiple environmental cues (Brophy & Voigt 2014). For example, Levskaya *et al* (2005) engineered E. coli a light sensitive receptor (signal input) fused to a histidine kinase (signal processor) that drives the expression of *lacZ* (reporter), such that exposure to red light turns off gene expression. Traditionally, whole cell biosensors have been developed that can only sense relevant compounds which naturally enter the cell, hence there is a need to develop modular sensors on the cell surface (Daringer et al. 2014).

Bacteria sense extracellular signals by the interaction of an input signal with outer membrane receptors (Figure 1.1A) or by the transport of small molecules into the cell which interact with an input sensor within the cell (Figure 1.1B). One example of an outer membrane receptor is OprF of the opportunistic pathogen *Pseudomonas aeruginosa* which uses the outer membrane protein, to bind the host derived inflammatory cytokine, IFN-γ, produced during inflammation (Wu et al. 2005). Binding of IFN-γ to OprF informs *P. aeruginosa* of the host's immune function and induces the production of type 1 *P. aeruginosa* lectin, facilitating pathogen adherence to epithelial cells and inducing barrier dysfunction (Wu et al. 2003). The intermediate processing step of IFN-γ binding to the outer membrane and induction of a response within the cell is not characterized at this time.

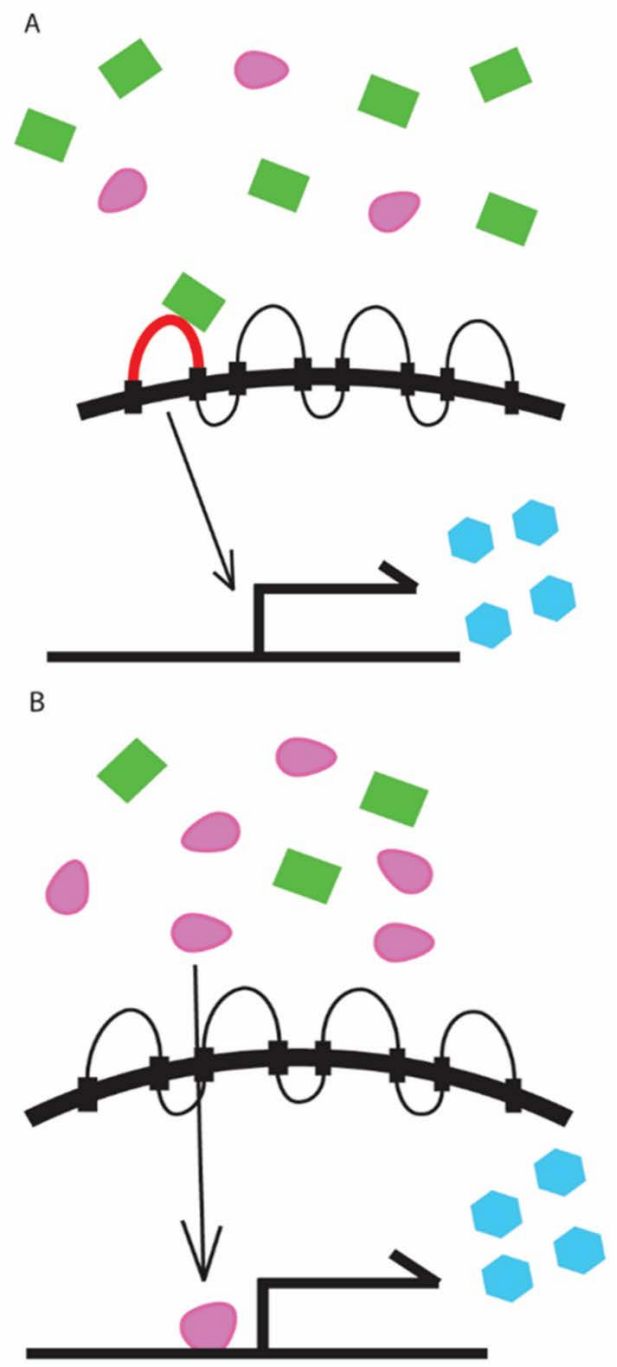

Figure 1.1: Bacterial processing of extracellular signals. (A) Extracellular signal interacts with a membrane receptor and the signal is transduced into the cell, activating a cellular response, (B) Extracellular signal enters the cell and interacts with the signal receptor in the periplasm or cytoplasm producing a cellular response.

There are two means in which the interaction of an extracellular signal with an outer membrane proteins is processed into a cellular response within the cell. The first method, is the use of a two-component regulatory systems (Mitrophanov & Groisman 2008). For example, the two-component osmosesnor system EnvZ- OmpR of *E. coli* has been well characterized. The transmembrane sensor, EnvZ consists of a sensor domain which resides in the periplasm and a cytoplasmic domain that interacts with the response regulator, OmpR (Baumgartner et al. 1994). The cytoplasm portion of EnvZ, a histidine kinase which transduces changes in extracellular osmolarity into an output signal by altering the phosphorylation, OmpR. The state of phosphorylation alters the conformation of OmpR, subsequently controlling the transcriptional regulation of the outer membrane porins OmpF and OmpC by affecting interaction of OmpR with the gene promoter (Baumgartner et al. 1994; Jin & Inouye 1993). Two component regulatory systems have been used in synthetic biology for the development of environmental bioreporters. A previous study achieved this using the intracellular domain of EnvZ fused to the receptor domain of the chemotaxis sensor, Tar (aspartate) (Michalodimitrakis et al. 2005; Baumgartner et al. 1994). A reporter was constructed using the OmpC promoter to express GFP, such that the system could differentiate, with high sensitivity between amino acids, some amino acids repressed expression while aspartate induced expression (Michalodimitrakis et al. 2005).

A second method in which extracellular signals are processed into cellular responses are stress response systems. The phage shock protein (*psp*) operon of *E. coli* responds to extracellular cues and manages their impact on the cell membrane (Darwin 2005). The *psp* operon can be induced by filamentous phage infection,

extreme temperatures, osmolarity, ethanol, and proton ionophores (Model et al. 1997). The *psp* operon consists of the sensor proteins; PspB/PspC located in the inner membrane which transduce the signal to the expression regulator, PspA located on the cytoplasmic surface of the inner membrane (Darwin 2005). Under non-induced conditions PspA negatively regulates the *psp* operon by binding the transcriptional activator, PspF (Weiner et al. 1991). Under stressed conditions PspF is released from PspA to activate transcription of *pspABCDE* and PspA aggregates at the inner membrane to prevent proton leakage (Kobayashi et al. 2007). The *pspA* promoter has been used as a reporter for phage infection and ethanol (Bergler et al. 1994).

For small molecules which are taken up by bacteria from the environment and activate metabolic pathways such as uric acid activation of the purine catabolic pathway of *Bacillus subtilis* can be harnessed for the monitoring of environmental cues. The *pucJKLM* operon of *B. subtilis* is involved in the uptake and degradation of uric acid under control of the transcriptional regulator, *pucR* (Schultz et al. 2001). When the transcriptional activator pucR is bound to uric acid or one of its degradation products, allantoin or allantoic acid it exhibits binding location-dependent transcriptional regulation of the *pucJKLM* operon while negatively regulating *pucR* expression (Beier et al. 2002). The transcriptional regulators of the presented signal transduction systems can be engineered to control the expression of a reporter gene in order to produce a quantifiable cellular response to an environmental stimulant.

Reporters

Transduction of an extracellular cue into a quantifiable signal by means of a reporter is necessary for the development of a bioreporter system and there are

numerous genetic reporters to select from. Transcriptional reporters are constructed such that the promoter of the gene induced by the signal processing element is placed upstream of a reporter gene. The most frequently used reporter genes are *lacZ*, *lux*, or *gfp* of which each has advantages and disadvantages.

Reporters encoded by *lacZ* (β-galactosidase) and the *lux* operon (luciferase) require the addition of a substrate and cell lysis, to produce a measurable readout (Robbens et al. 2010). The β-galactosidase assay is widely used and well characterized for the measurement of promoter activity. β-galactosidase activity is measured by cleavage of o-nitrophenol-β-D-galactopyranoside into galactose and o-nitrophenol producing a yellow color. However, the use of a fluorometric substrate such as methyllumbelliferyl-β-D-galactopyranoside substantially increases the sensitivity of the assay, up to three orders of magnitude relative to the colorimetric substrate (Gutiérrez et al. 2015). Luciferase (*luxAB*) requires the addition of luciferin and cell lysis in order to measure gene activity, however, it is one of the most sensitive methods for measuring transcriptional activity (Close et al. 2012).

A GFP based reporter is commonly used when a substrate independent reporter is necessary and does not require cell lysis giving it a distinct advantage. However, GFP requires a longer time to reach fluorescence levels that permit differentiation between gene expression and is quite stable (Sørensen et al. 2006). The reporter must be selected carefully taking into consideration the need for sensitivity, stability and response speed, in order to develop a whole cell biosensor capable of working in the developed system.

Identification of individual receptors and subsequent regulated promoters for

environmental cues is necessary for the development of novel sensor circuits for monitoring and treating non-communicable diseases. Characterization and development of novel circuits adds to the repertoire of available components that can be used individually or in combination for the detection of disease markers. The majority of sensors developed have been limited to molecules that are actively transported or diffuse into the bacterial cell, for example, there have been numerous whole cell bioreporters developed for detecting toxic compounds such as arsenic (Stocker et al. 2003) or Cu^{2+} (Shetty et al. 2004). However, there are limited examples of surface receptors developed for detection of environmental factors or ligands. Though, Daringer *et al* (2014) developed a modular and tunable extracellular mammalian circuit system termed, MESA (modular extracellular sensor architecture). MESA, consists of a modular extracellular receptor which can be tailored to a ligand and either outputs a transcription factor or enzymes based on the application. The modularity and tunability of extracellular sensors allows the development of new sensor that can be combined with other circuits for the processing of multiple signals by an individual cell. Commensal bacteria could be used to deploy these sensors in the gastrointestinal tract to monitor disease related conditions, further, deployment would not necessarily be limited to the intestine (Goh et al. 2012).

Synthetically biology has produced systems for a multitude of application from whole cell heavy metal biosensors, to engineered metabolic pathways for the production of value added compounds. Nevertheless, the majority of systems developed for therapeutic applications have been proofs of concept at the bench scale. The Fussenegger group has developed multiple mammalian systems that detect

environmental cues and respond, for example, they developed a uric acid regulatory device which monitored blood concentrations. The system remained off at physiologically normal concentrations of uric acid, however, under elevated conditions, the cells produced urate oxidase to reduce uric acid concentration in a dose dependent manner, returning uric acid concentrations to a homeostatic concentration (Kemmer et al. 2010).

Prokaryotic systems have been developed to monitor and record the presence of anhydrotetracycline during transit through the mouse gastrointestinal tract (Kotula et al. 2014). Another system developed by Hwang *et al* (2014), *E. coli* was engineered to sense the quorum sensing molecule, N-Acyl homoserine lactone (AHL) produced by *P. aeruginosa* and swim towards the pathogen by following the AHL gradient. Detection of AHL induced the production of microsin S and DNaseI which were secreted to degrade biofilms and kill *P. aeruginosa* (Saeidi et al. 2011; Hwang et al. 2014). These two studies provide useful systems for the development of active therapeutics to be deployed in the gastrointestinal tract.

Bacteria based therapeutic systems that have been developed for use in the gastrointestinal tract have mainly consisted of an engineered probiotic which constitutively expresses a therapeutic agent. For example, Duan *et al* (2015) of our lab, engineered the commensal bacteria, *Lactobacillus gasseri* to constitutively secrete GLP-1 (1-37). Oral administration of the engineered strain to diabetic rats resulted in conversion some epithelial cells into glucose responsive insulin secreting cells for the treatment of hyperglycemia. Currently, there are no prokaryotic based therapeutics approved by the FDA. However, Intrexon® has successfully completed a Phase 2a

trial for AG011 which consists of oral administration of *Lactococcus lactis* engineered to secrete interleukin-10 for the treatment of ulcerative colitis. With the progression of engineered prokaryotic treatments of inflammatory based diseases, there is a need to develop sensors which are capable of monitoring extracellular inflammatory markers to expand the available tools to detect disease biomarkers and respond.

The capacity of *P. aeruginosa* to bind and respond to IFN-γ inspired us to develop a novel synthetic receptor for IFN-γ, expressed in *E. coli*. Identification of the peptide fragment(s) of OprF which bind IFN-γ was necessary to develop a fusion protein such that the extracellular loops of OmpA were replaced with the identified peptide fragment(s) of OprF to yield a sensor. A reporter was constructed using the CpxA/CpxR two-component regulatory system, which had been previously identified to respond to interactions of OmpA with extracellular stimuli (Ma & Wood 2009). However, the CpxA/CpxR based reporter did not produce a response to IFN-γ binding to the based OmpA/OprF receptor. Therefore, a novel reporter construct was developed using the *pspA* stress response promoter. The detection system was characterized and the capacity of the system to detect IFN-γ and TNF-α in an IBD *in vitro* model was examined. Secondly, a system for the detection of uric acid was developed by implementing components of the purine catabolism system of *B. subtilis*. A synthetic promoter was developed as a reporter for uric acid in which the transcriptional regulator, *pucR* bound to uric acid regulates the expression of the synthetic promoter. These novel bioreporter systems will add new circuits to select from for the development of environmentally aware therapeutics for monitoring and treating disease. These novel bioreporters can be used for the detection of biomarkers

of individual diseases such as IBD and gout or the responses can be integrated into more complex circuits such as and gates for the detection of other diseases such as cardiovascular disease.

References

References

Al-Sadi R, Boivin M, Ma T. 2009.,Mechanism of cytokine modulation of epithelial tight junction barrier. *Front. Biosci.* **14**:2765–2778. http://www.ncbi.nlm.nih.gov/pmc/articles/PMC3724223/.

Ancker JS, Witteman HO, Hafeez B, Provencher T, Van de Graaf M, Wei E. 2015.,"You Get Reminded You're a Sick Person": Personal Data Tracking and Patients With Multiple Chronic Conditions. *J. Med. Internet Res.* **17**:e202.

Arrieta MC, Bistritz L, Meddings JB. 2006.,Alterations in intestinal permeability. *Gut* **55**:1512–1520. http://www.ncbi.nlm.nih.gov/pmc/articles/PMC1856434/.

Aurand TC, Russell MS, March JC. 2012.,Synthetic signaling networks for therapeutic applications. *Curr. Opin. Biotechnol.* **23**:773–779. http://www.ncbi.nlm.nih.gov/pubmed/22285057.

Ausländer S, Fussenegger M. 2013.,From gene switches to mammalian designer cells: present and future prospects. *Trends Biotechnol.* **31**:155–168. http://www.sciencedirect.com/science/article/pii/S0167779912002016.

Baumgartner JW, Kim C, Brissette RE, Inouye M, Park C, Hazelbauer GL. 1994.,Transmembrane signalling by a hybrid protein: communication from the domain of chemoreceptor Trg that recognizes sugar-binding proteins to the kinase/phosphatase domain of osmosensor EnvZ. *J. Bacteriol.* **176** :1157–1163. http://jb.asm.org/content/176/4/1157.abstract.

Beier L, Nygaard P, Jarmer H, Saxild HH. 2002.,Transcription Analysis of the Bacillus subtilis PucR Regulon and Identification of a cis-Acting Sequence Required for PucR-Regulated Expression of Genes Involved in Purine Catabolism. *J. Bacteriol.* **184** :3232–3241. http://jb.asm.org/content/184/12/3232.abstract.

Benner SA. 2003.,Synthetic biology: Act natural. *Nature* **421**:118.

http://dx.doi.org/10.1038/421118a.

Bergler H, Abraham D, Aschauer H, Turnowsky F. 1994.,Inhibition of lipid biosynthesis induces the expression of the pspA gene. *Microbiology* **140 (Pt 8**:1937–44. http://mic.microbiologyresearch.org/content/view.action?itemId=http%3A%2F%2Fsgm.metastore.ingenta.com%2Fcontent%2Fjournal%2Fmicro%2F10.1099%2F13500872-140-8-1937&view=&itemType=http%3A%2F%2Fpub2web.metastore.ingenta.com%2Fns%2FArticle.

Bhole V, Choi JWJ, Woo Kim S, de Vera M, Choi H. 2015.,Serum Uric Acid Levels and the Risk of Type 2 Diabetes: A Prospective Study. *Am. J. Med.* **123**:957–961. http://dx.doi.org/10.1016/j.amjmed.2010.03.027.

Bischoff SC, Barbara G, Buurman W, Ockhuizen T, Schulzke J-D, Serino M, Tilg H, Watson A, Wells JM. 2014.,Intestinal permeability -- a new target for disease prevention and therapy. *BMC Gastroenterol.* **14**:1–25. http://dx.doi.org/10.1186/s12876-014-0189-7.

Bisping G, Lügering N, Lütke-Brintrup S, Pauels H-G, Schürmann G, Domschke W, Kucharzik T. 2001.,Patients with inflammatory bowel disease (IBD) reveal increased induction capacity of intracellular interferon-gamma (IFN-γ) in peripheral CD8+ lymphocytes co-cultured with intestinal epithelial cells. *Clin. Exp. Immunol.* **123**:15–22. http://dx.doi.org/10.1046/j.1365-2249.2001.01443.x.

Braegger CP, Nicholls S, Murch SH, MacDonald TT, Stephens S. 1992.,Tumour necrosis factor alpha in stool as a marker of intestinal inflammation. *Lancet* **339**:89–91. http://www.sciencedirect.com/science/article/pii/0140673692909 99J.

Brophy JAN, Voigt CA. 2014.,Principles of genetic circuit design. *Nat Meth* **11**:508–520. http://dx.doi.org/10.1038/nmeth.2926.

Cameron DE, Bashor CJ, Collins JJ. 2014.,A brief history of synthetic biology. *Nat Rev Micro* **12**:381–390. http://dx.doi.org/10.1038/nrmicro3239.

Carty E, De Brabander M, Feakins RM, Rampton DS. 2000.,Measurement of in vivo rectal mucosal cytokine and eicosanoid production in ulcerative colitis using filter paper. *Gut* **46** :487–492. http://gut.bmj.com/content/46/4/487.abstract.

Clarke MB, Hughes DT, Zhu C, Boedeker EC, Sperandio V. 2006.,The QseC sensor kinase: A bacterial adrenergic receptor. *Proc. Natl. Acad. Sci.* **103** :10420–10425. http://www.pnas.org/content/103/27/10420.abstract.

Close D, Xu T, Smartt A, Rogers A, Crossley R, Price S, Ripp S, Sayler G. 2012.,The Evolution of the Bacterial Luciferase Gene Cassette (lux) as a Real-Time Bioreporter. *Sensors (Basel).* **12**:732–752. http://www.ncbi.nlm.nih.gov/pmc/articles/PMC3279237/.

Daringer NM, Dudek RM, Schwarz KA, Leonard JN. 2014.,Modular Extracellular Sensor Architecture for Engineering Mammalian Cell-based Devices. *ACS Synth. Biol.* **3**:892–902. http://www.ncbi.nlm.nih.gov/pmc/articles/PMC4161666/.

Darwin AJ. 2005.,The phage-shock-protein response. *Mol. Microbiol.* **57**:621–628. http://dx.doi.org/10.1111/j.1365-2958.2005.04694.x.

Drago S, El Asmar R, Di Pierro M, Grazia Clemente M, Sapone ATA, Thakar M, Iacono G, Carroccio A, D'Agate C, Not T, Zampini L, Catassi C, Fasano A. 2006.,Gliadin, zonulin and gut permeability: Effects on celiac and non-celiac intestinal mucosa and intestinal cell lines. *Scand. J. Gastroenterol.* **41**:408–419. http://www.tandfonline.com/doi/abs/10.1080/00365520500235334.

Duan FF, Liu JH, March JC. 2015.,Engineered Commensal Bacteria Reprogram Intestinal Cells Into Glucose-Responsive Insulin-Secreting Cells for the Treatment of Diabetes. *Diabetes* **64**:1794–1803. http://diabetes.diabetesjournals.org/lookup/doi/10.2337/db14-0635.

Enocksson A, Lundberg J, Weitzberg E, Norrby-Teglund A, Svenungsson B. 2004.,Rectal Nitric Oxide Gas and Stool Cytokine Levels during the Course of Infectious Gastroenteritis. *Clin. Diagn. Lab. Immunol.* **11**:250–254. http://www.ncbi.nlm.nih.gov/pmc/articles/PMC371199/.

Fish SM, Proujansky R, Reenstra WW. 1999.,Synergistic effects of interferon γ and tumour necrosis factor α on T84 cell function. *Gut* **45** :191–198. http://gut.bmj.com/content/45/2/191.abstract.

Gerteis J, Izrael D, Deitz D, LeRoy L, Ricciardi R, Miller T, Basu J. 2014.,Multiple Chronic Conditions Chartbook. *AHRQ*. http://www.ahrq.gov/sites/default/files/wysiwyg/professionals/prevention-chronic-care/decision/mcc/mccchartbook.pdf.

Goh Y-L, He H, March JC. 2012.,Engineering commensal bacteria for prophylaxis against infection. *Curr. Opin. Biotechnol.* **23**:924–930. http://www.sciencedirect.com/science/article/pii/S0958166912000511.

Gutiérrez JC, Amaro F, Martín-González A. 2015.,Heavy metal whole-cell biosensors using eukaryotic microorganisms: an updated critical review. *Front. Microbiol.* **6**:48. http://www.ncbi.nlm.nih.gov/pmc/articles/PMC4335268/.

Hosomi A, Nakanishi T, Fujita T, Tamai I. 2012.,Extra-Renal Elimination of Uric Acid via Intestinal Efflux Transporter BCRP/ABCG2. *PLoS One* **7**:e30456. http://dx.doi.org/10.1371%2Fjournal.pone.0030456.

Hwang IY, Tan MH, Koh E, Ho CL, Poh CL, Chang MW. 2014.,Reprogramming Microbes to Be Pathogen-Seeking Killers. *ACS Synth. Biol.* **3**:228–237. http://dx.doi.org/10.1021/sb400077j.

Ito R, Shin-Ya M, Kishida T, Urano A, Takada R, Sakagami J, Imanishi J, Kita M, Ueda Y, Iwakura Y, Kataoka K, Okanoue T, Mazda O. 2006.,Interferon-gamma is causatively involved in experimental inflammatory bowel disease in mice. *Clin. Exp. Immunol.* **146**:330–338. http://dx.doi.org/10.1111/j.1365-2249.2006.03214.x.

Jacob F, Monod J. 1961.,On the regulation of gene activity. In: . *Cold Spring Harb. Symp. Quant. Biol.* Cold Spring Harbor Laboratory Press, Vol. 26, pp. 193–211.

Jin T, Inouye M. 1993.,Ligand Binding to the Receptor Domain Regulates the Ratio of

Kinase to Phosphatase Activities of the Signaling Domain of the Hybrid Escherichia coli Transmembrane Receptor, Taz1. *J. Mol. Biol.* **232**:484–492. http://www.sciencedirect.com/science/article/pii/S002228368371404X.

Kemmer C, Gitzinger M, Daoud-El Baba M, Djonov V, Stelling J, Fussenegger M. 2010.,Self-sufficient control of urate homeostasis in mice by a synthetic circuit. *Nat Biotech* **28**:355–360. http://dx.doi.org/10.1038/nbt.1617.

Kobayashi R, Suzuki T, Yoshida M. 2007.,Escherichia coli phage-shock protein A (PspA) binds to membrane phospholipids and repairs proton leakage of the damaged membranes. *Mol. Microbiol.* **66**:100–109. http://dx.doi.org/10.1111/j.1365-2958.2007.05893.x.

Kotula JW, Kerns SJ, Shaket LA, Siraj L, Collins JJ, Way JC, Silver PA. 2014.,Programmable bacteria detect and record an environmental signal in the mammalian gut. *Proc. Natl. Acad. Sci.* **111** :4838–4843. http://www.pnas.org/content/111/13/4838.abstract.

Kutzing MK, Firestein BL. 2008.,Altered Uric Acid Levels and Disease States. *J. Pharmacol. Exp. Ther.* **324** :1–7. http://jpet.aspetjournals.org/content/324/1/1.abstract.

Lainscak M, von Haehling S, Anker SD. 2009.,Natriuretic peptides and other biomarkers in chronic heart failure: from BNP, NT-proBNP, and MR-proANP to routine biochemical markers. *Int. J. Cardiol.* **132**:303–11. http://www.ncbi.nlm.nih.gov/pubmed/19144431.

Lallès J-P. 2015.,Intestinal Alkaline Phosphatase in Stool: A Novel Biomarker for Metabolic Diseases. *EBioMedicine*. http://www.sciencedirect.com/science/article/pii/S2352396415001899.

Levskaya A, Chevalier AA, Tabor JJ, Simpson ZB, Lavery LA, Levy M, Davidson EA, Scouras A, Ellington AD, Marcotte EM, Voigt CA. 2005.,Synthetic biology: Engineering Escherichia coli to see light. *Nature* **438**:441–442. http://dx.doi.org/10.1038/nature04405.

Luck SN, Bennett-Wood V, Poon R, Robins-Browne RM, Hartland EL. 2005.,Invasion of Epithelial Cells by Locus of Enterocyte Effacement-Negative Enterohemorrhagic Escherichia coli . *Infect. Immun.* **73**:3063–3071. http://www.ncbi.nlm.nih.gov/pmc/articles/PMC1087320/.

Ma Q, Wood TK. 2009.,OmpA influences Escherichia coli biofilm formation by repressing cellulose production through the CpxRA two-component system. *Environ. Microbiol.* **11**:2735–2746. http://dx.doi.org/10.1111/j.1462-2920.2009.02000.x.

Ma TY, Iwamoto GK, Hoa NT, Akotia V, Pedram A, Boivin MA, Said HM. 2004.,TNF-α-induced increase in intestinal epithelial tight junction permeability requires NF-κB activation. *Am. J. Physiol. - Gastrointest. Liver Physiol.* **286**:G367–G376. http://ajpgi.physiology.org/content/286/3/G367.abstract.

MacDonald TT, Hutchings P, Choy MY, Murch S, Cooke A. 1990.,Tumour necrosis factor-alpha and interferon-gamma production measured at the single cell level in normal and inflamed human intestine. *Clin. Exp. Immunol.* **81**:301–305. http://www.ncbi.nlm.nih.gov/pmc/articles/PMC1535044/.

Madara JL, Stafford J. 1989.,Interferon-gamma directly affects barrier function of cultured intestinal epithelial monolayers. *J. Clin. Invest.* **83**:724–727. http://www.ncbi.nlm.nih.gov/pmc/articles/PMC303735/.

Madsen K, Cornish A, Soper P, McKaigney C, Jijon H, Yachimec C, Doyle J, Jewell L, De Simone C. 2001.,Probiotic bacteria enhance murine and human intestinal epithelial barrier function. *Gastroenterology* **121**:580–591. http://www.sciencedirect.com/science/article/pii/S0016508501903269.

Mendis. S, Armstrong T, Bettcher D, Branca F, Lauer J, Mace C, Poznyak V, Riley L, Silva VDCE, Stevens G. 2014.,Global Status Report on Noncommunicable Disease 2014. *World Heal. Organ.* http://apps.who.int/iris/bitstream/10665/148114/1/9789241564854_eng.pdf?ua=1 .

Michalodimitrakis KM, Sourjik V, Serrano L. 2005.,Plasticity in amino acid sensing of the chimeric receptor Taz. *Mol. Microbiol.* **58**:257–266. http://dx.doi.org/10.1111/j.1365-2958.2005.04821.x.

Mitrophanov AY, Groisman EA. 2008.,Signal integration in bacterial two-component regulatory systems. *Genes Dev.* **22**:2601–2611. http://www.ncbi.nlm.nih.gov/pmc/articles/PMC2751022/.

Model P, Jovanovic G, Dworkin J. 1997.,The Escherichia coli phage-shock-protein (psp) operon. *Mol. Microbiol.* **24**:255–261. http://dx.doi.org/10.1046/j.1365-2958.1997.3481712.x.

Neurath MF. 2014.,Cytokines in inflammatory bowel disease. *Nat Rev Immunol* **14**:329–342. http://dx.doi.org/10.1038/nri3661.

Nguyen Y, Sperandio V. 2012.,Enterohemorrhagic E. coli (EHEC) pathogenesis. *Front. Cell. Infect. Microbiol.* **2**:90. http://www.ncbi.nlm.nih.gov/pmc/articles/PMC3417627/.

Ogura J, Kuwayama K, Takaya A, Terada Y, Tsujimoto T, Koizumi T, Maruyama H, Fujikawa A, Takahashi N, Kobayashi M. 2012.,Intestinal ischemia-reperfusion increases efflux for uric acid via paracellular route in the intestine, but decreases that via transcellular route mediated by BCRP. *J. Pharm. Pharm. Sci.* **15**:295–304.

Papadakis KA, Targan SR. 2000.,Role of Cytokines in the Pathogenesis of Inflammatory Bowel Disease. *Annu. Rev. Med.* **51**:289–298. http://dx.doi.org/10.1146/annurev.med.51.1.289.

Pearson TA, Mensah GA, Alexander RW, Anderson JL, Cannon RO, Criqui M, Fadl YY, Fortmann SP, Hong Y, Myers GL, Rifai N, Smith SC, Taubert K, Tracy RP, Vinicor F. 2003.,Markers of Inflammation and Cardiovascular Disease: Application to Clinical and Public Health Practice: A Statement for Healthcare Professionals From the Centers for Disease Control and Prevention and the American Heart Association . *Circ.* **107** :499–511.

http://circ.ahajournals.org/content/107/3/499.short.

Progress M, Feig DI, Kang D, Johnson RJ, Haig A, Davis NS. 2008.,Uric Acid and Cardiovascular Risk.

Rescigno M. 2011.,The intestinal epithelial barrier in the control of homeostasis and immunity. *Trends Immunol.* **32**:256–264. http://www.sciencedirect.com/science/article/pii/S1471490611000585.

Robbens J, Dardenne F, Devriese L, De Coen W, Blust R. 2010.,Escherichia coli as a bioreporter in ecotoxicology. *Appl. Microbiol. Biotechnol.* **88**:1007–1025.

Robinson K, Deng Z, Hou Y, Zhang G. 2015.,Regulation of the Intestinal Barrier Function by Host Defense Peptides. *Front. Vet. Sci.* **2**:57. http://www.ncbi.nlm.nih.gov/pmc/articles/PMC4672242/.

Saeidi N, Wong CK, Lo T, Nguyen HX, Ling H, Leong SSJ, Poh CL, Chang MW. 2011.,Engineering microbes to sense and eradicate Pseudomonas aeruginosa, a human pathogen. *Mol. Syst. Biol.* **7**. http://msb.embopress.org/content/7/1/521.abstract.

Schultz AC, Nygaard P, Saxild HH. 2001.,Functional Analysis of 14 Genes That Constitute the Purine Catabolic Pathway in Bacillus subtilis and Evidence for a Novel Regulon Controlled by the PucR Transcription Activator. *J. Bacteriol.* **183** :3293–3302. http://jb.asm.org/content/183/11/3293.abstract.

Shetty RS, Deo SK, Liu Y, Daunert S. 2004.,Fluorescence-based sensing system for copper using genetically engineered living yeast cells. *Biotechnol. Bioeng.* **88**:664–670. http://dx.doi.org/10.1002/bit.20331.

Sorensen LB. 1965.,Role of the intestinal tract in the elimination of uric acid. *Arthritis Rheum.* **8**:694–706. http://www.ncbi.nlm.nih.gov/pubmed/5859543.

Sørensen SJ, Burmølle M, Hansen LH. 2006.,Making bio-sense of toxicity: new developments in whole-cell biosensors. *Curr. Opin. Biotechnol.* **17**:11–16. http://www.sciencedirect.com/science/article/pii/S0958166905001990.

Spencer DM, Veldman GM, Banerjee S, Willis J, Levine AD. 2002.,Distinct inflammatory mechanisms mediate early versus late colitis in mice. *Gastroenterology* **122**:94–105. http://www.sciencedirect.com/science/article/pii/S0016508502653715.

Sperandio V, Torres AG, Jarvis B, Nataro JP, Kaper JB. 2003.,Bacteria–host communication: The language of hormones. *Proc. Natl. Acad. Sci.* **100** :8951–8956. http://www.pnas.org/content/100/15/8951.abstract.

Stocker J, Balluch D, Gsell M, Harms H, Feliciano J, Daunert S, Malik KA, van der Meer JR. 2003.,Development of a Set of Simple Bacterial Biosensors for Quantitative and Rapid Measurements of Arsenite and Arsenate in Potable Water. *Environ. Sci. Technol.* **37**:4743–4750. http://dx.doi.org/10.1021/es034258b.

Ulluwishewa D, Anderson RC, McNabb WC, Moughan PJ, Wells JM, Roy NC. 2011.,Regulation of Tight Junction Permeability by Intestinal Bacteria and Dietary Components. *J. Nutr.* **141** :769–776. http://jn.nutrition.org/content/141/5/769.abstract.

Ward BW, Schiller JS, Goodman RA. 2014.,Multiple Chronic Conditions Among US Adults: A 2012 Update. *Prev. Chronic Dis.* **11**:E62. http://www.ncbi.nlm.nih.gov/pmc/articles/PMC3992293/.

Watson CJ, Rowland M, Warhurst G. 2001.,Functional modeling of tight junctions in intestinal cell monolayers using polyethylene glycol oligomers. *Am. J. Physiol. - Cell Physiol.* **281**:C388–C397. http://ajpcell.physiology.org/content/281/2/C388.abstract.

Watson CJ, Hoare CJ, Garrod DR, Carlson GL, Warhurst G. 2005.,Interferon-γ selectively increases epithelial permeability to large molecules by activating different populations of paracellular pores. *J. Cell Sci.* **118** :5221–5230. http://jcs.biologists.org/content/118/22/5221.abstract.

Weiner L, Brissette JL, Model P. 1991.,Stress-induced expression of the Escherichia coli phage shock protein operon is dependent on sigma 54 and modulated by

positive and negative feedback mechanisms. *Genes Dev.* **5** :1912–1923. http://genesdev.cshlp.org/content/5/10/1912.abstract.

Wu L, Estrada O, Zaborina O, Bains M, Shen L, Kohler JE, Patel N, Musch MW, Chang EB, Fu Y-X, Jacobs MA, Nishimura MI, Hancock REW, Turner JR, Alverdy JC. 2005.,Recognition of Host Immune Activation by Pseudomonas aeruginosa. *Science (80-.).* **309**:774–777. http://www.sciencemag.org/content/309/5735/774.abstract.

Wu L, Holbrook C, Zaborina O, Ploplys E, Rocha F, Pelham D, Chang E, Musch M, Alverdy J. 2003.,Pseudomonas aeruginosa Expresses a Lethal Virulence Determinant, the PA-I Lectin/Adhesin, in the Intestinal Tract of a Stressed Host: The Role of Epithelia Cell Contact and Molecules of the Quorum Sensing Signaling System. *Ann. Surg.* **238**:754–764. http://www.ncbi.nlm.nih.gov/pmc/articles/PMC1356156/.

CHAPTER TWO

Development of a Synthetic Receptor Protein for Sensing Inflammatory Mediators Interferon-γ and Tumor Necrosis Factor-α*

* *Published*: *Aurand TC, March JC. Development of a synthetic receptor protein for sensing inflammatory mediators interferon-γ and tumor necrosis factor-α. Biotechnol Bioeng. 2016;113(3):492–500* *Reprinted with permission.*

Abstract

Intestinal inflammation has been implicated in a number of diseases, including diabetes, Crohn's disease and irritable bowel syndrome. Important components of inflammation are interferon-γ (IFN-γ) and tumor necrosis factor-α (TNF-α), which are elevated both on the luminal and submucosal sides of the intestinal epithelial barrier in several diseases. Here, we developed a novel *E. coli* based detection system for IFN-γ and TNF-α comprised of a chimeric protein and a simple signal transduction construct, which could be deployed on the luminal side of the intestine. OmpA of *E. coli* was engineered to detect IFN-γ or TNF-α through the replacement of extracellular loops with peptide fragments from OprF of *P. aeruginosa*. OmpA/OprF chimeras were developed, capable of binding IFN-γ or TNF-α. The specific peptide fragments that bind IFN-γ were identified. IFN-γ or TNF-α binding the OmpA/OprF chimera induced the *pspA* promoter, driving β-galactosidase production. The OmpA/OprF chimera had a detection limit of 300 pM for IFN-γ and 150 pM for TNF-α. The detection limit of 150 pM for TNF-α is within the physiological disease concentrations observed in the stool of IBD patients (15.9-343.8 pM). This work will further the development of bacteria based therapeutics for the treatment of inflammatory diseases of the gut.

Introduction

Communication between commensal and pathogenic microorganisms with their hosts has evolved over millions of years. Some microorganisms have the capability to detect and respond to host hormonal and cytokine signals (Hughes & Sperandio 2008). For example, the food-borne pathogen enterohemorrhagic

Escherichia coli O157:H7, senses host-produced adrenaline and noradrenaline or the microbiota derived signal, autoinducer-3 (AI-3), to determine the environment and activate virulence genes (Sperandio et al. 2003; Clarke et al. 2006). The opportunistic pathogen *Pseudomonas aeruginosa* (PAO1) detects interferon-γ (IFN-γ), an inflammatory T cell derived cytokine, through the binding of IFN-γ to the outer membrane protein OprF, in turn, inducing transcription of *rhlI* (Ding et al. 2010; Wu et al. 2005). Upon sensing IFN-γ, PAO1 induces type 1 *P. aeruginosa* lectin (PA-1) production through quorum sensing, altering the permeability of the intestinal epithelium (Wu et al. 2005; Laughlin et al. 2000).

A bacteria based detection system harnessing pathogenic mechanisms for detecting the host's condition must be engineered in a non-pathogenic, native gut bacteria such as *E. coli,* if it is to be deployed in humans (Aurand et al. 2012; Goh et al. 2012). Probiotics can be engineered as therapeutics for the treatment of disease. An example developed in our lab employed engineered commensal bacteria for the treatment of diabetes (Duan et al. 2008). Treatment of type 1 diabetic rats with the engineered *L. gasseri* produced 60% more total insulin through reprogrammed endocrine cells in the intestine (Duan et al. 2015). The use of engineered probiotics as a delivery vehicle for therapeutics allows for targeting of specific regions of the gastrointestinal tract. Further, there are already strains of *E. coli* (such as Nissle 1917) that are commercially available as over-the-counter probiotics. Therefore, *E. coli* was selected to engineer a detection system for the inflammation marker IFN-γ that incorporates aspects of the outer membrane porin OprF of *P. aeruginosa*. Binding of IFN-γ to OprF and subsequent signal transduction between OprF and the *rhl* quorum

sensing system has not been fully characterized and, therefore, the system could not be reproduced in its entirety in *E. coli*.

The outer membrane porin, OmpA of *E. coli* shares homology to OprF, has been well characterized and is used for surface display of peptides (Verhoeven et al. 2009; Khalid et al. 2006). OmpA and OprF consist of two domains: the N-terminal domain forms an eight-stranded antiparallel transmembrane β-barrel with four extracellular loops, and a C-terminal periplasmic domain (Pautsch & Schulz 2000; Khalid et al. 2006). However, OprF exists in two conformations: approximately 96% as a two domain conformation and 4% form a single domain 16-stranded β-barrel (Sugawara et al. 2006). There are two proposed secondary-structure models of OprF as a single domain conformation: one proposed by Rawling *et al.* (1995) and an alternate model proposed by Gilleland *et al.* (1995) (Fig. 2.1). In both models there are eight extracellular loops. However, the two models differ in the size of the fifth loop. In the Rawling model (1995), the fifth loop consists of a larger (52 amino acid) surface exposed region, whereas the Gilleland model's (1995) fifth loop contains only 17 amino acids (Fig. 2.1). The smaller fifth loop of the Gilleland model shifts the surface exposed amino acids of loop 6 relative to the Rawling model as can be seen in Figure 2.1 (shaded regions). Peptides pertaining to loops 7 and 8 of both models elicit an immunogenic response (Gilleland Jr. et al. 1995; Hughes et al. 1992).

Figure 2.1: Alignment of OprF such that secondary extracellular loop structures proposed by Rawling *et al*. (1995) (top sequence) or Gilleland *et al*. (1995) (bottom sequence) are colored. Loops identified by the Gilleland (1995) model are identified with an *. Loops 1-4 constitute the N-terminal domain of the two domain conformation of OprF, and loops 1-8 constitute the large single domain conformation of OprF.

OmpA and OprF are orthologs with similar predicted secondary structure making OmpA a suitable candidate for engineering a chimeric protein that imparts *P. aeruginosa* IFN-γ detection capacity to *E. coli*. Additionally, OmpA is relatively abundant (approximately 100,000 copies/cell), and capable of folding into a similar structure to the wild type upon replacement or deletion of extracellular loops (Koebnik et al. 2000; Koebnik 1999).

The development of a detection system for biomarkers such as IFN-γ requires a sensor, signal transduction and a reporter. Here, we investigate the Phage shock protein (Psp) system as a signal transduction mediator. The Psp stress response system of *E. coli* is a conserved system that detects extracellular stress and transduces outer membrane stress to receptors on the inner membrane, PspB and PspC, and induces PspA. The mechanism of signal transduction between the outer membrane and the inner membrane has not been clearly defined (Joly et al. 2010). Under non-induced conditions, PspA negatively regulates the *Psp* operon by binding PspF (Weiner et al. 1991). The Psp system can be induced by filamentous phage infection, extreme temperatures, osmolarity, ethanol, and proton ionophores (Model et al. 1997). Under Psp-inducing conditions, PspF is released from the PspA/PspF inhibitory complex to activate transcription of *PspABCDE*.

In this work, we report on novel chimeric proteins made from sections of OmpA and OprF that are capable of binding the human inflammation cytokines IFN-γ and TNF-α. Furthermore, we investigated a method for transducing the binding event of IFN-γ to the OmpA/OprF chimera into the cell to mediate a measurable response.

Materials and Methods

Bacterial Strains

Host strains *E. coli* Dh5α and JW0940 (*ΔompA::kan*) (Baba et al. 2006) were used for recombinant DNA manipulation and protein expression respectively. *P. aeruginosa* PAO1 was used for the amplification of *oprF* and *E. coli* MG1655 was used for the amplification of *ompA* and *pspA*. Bacterial strains and plasmids used in this study are found in (Table 2.1). Strains were grown aerobically in Luria-Bertani (LB) broth at 37°C or 30°C, supplemented with appropriate antibiotics: chloramphenicol 12.5 μg/mL and tetracycline 10 μg/mL. Peptides used in this study were recombinant human IFN-γ Peprotech (Rocky Hill, NJ) and recombinant human TNF-α Shenandoah Biotechnology Inc. (Warwick, Pa).

Table 2.1: Bacterial strains and plasmids used in this study

Strains		Reference
Pseudomonas aeruginosa		
PAO1	Wild Type	Lab collection
Escherichia coli		
MG1655	F- lambda- *ilvG- rfb* -50 *rph* -1	Lab collection
JW0940	F-, Δ(araD-araB)567, ΔlacZ4787(::rrnB-3), λ-, ΔompA772::kan, rph-1, Δ(rhaD-rhaB)568, hsdR514	Baba et al, 2006
Dh5α	F-, endA1, hsdR17(rk2 mk+), supE44, thi-1, recA1, gyrA, relA1, D(lacZYA-argF)U169, deoR, W80 lacZDM15	Lab collection
BW25113	F^{-}, DE(araD-araB)567, lacZ4787(del)::rrnB-3, LAM^{-}, rph-1, DE(rhaD-rhaB)568, hsdR514	Lab collection
Plasmids		
pBAC-lacZ	CamR	Addgene plasmid #13422
pMR0107	TetR	Lab collection, pSC101 derivative
pTCA0	pSC101 containg OmpA, CamR	This study
pTCA1	pTCA0, OmpA (AA 38-54) replaced with OprF (AA 44-50)	This study
pTCA2	pTCA1, OmpA (AA 79-95) replaced with OprF (AA 77-87)	This study
pTCA3	pTCA2, OmpA (AA 125-137) replaced with OprF (AA 121-130)	This study
pTCA4	pTCA0, OmpA (AA 38-54) replaced with OprF (AA 198-237)	This study
pTCA5	pTCA0, OmpA (AA 79-95) replaced with OprF (AA 257-275)	This study
pTCA6	pTCA4, OmpA (AA 79-95) replaced with OprF (AA 257-275)	This study
pTCA7	pTCA6, OmpA (AA 125-137) replaced with OprF (AA 310-314)	This study
pTCA8	pTCA0, OmpA (AA 38-54) replaced with OprF (AA 200-217)	This study
pTCA9	pTCA0, OmpA (AA 79-95) replaced with OprF (AA 241-261)	This study
pTCA10	pTCA8, OmpA (AA 79-95) replaced with OprF (AA 241-261)	This study
pPALacZ1	pBAC-lacZ containg the PspA promoter and LacZ gene, CamR	This study

Plasmid construction

Target genes *ompA* of *E. coli* MG1655 and *oprF* of *P. aeruginosa* were PCR amplified from chromosomal DNA using Q5 High Fidelity Polymerase NEB (Ipswich, MA). Primers for the PCR fragments were designed, such that they had a minimum 15-bp homology at their ends for Gibson Assembly (Gibson et al. 2009). *ompA* and *oprF* with corresponding homology to the linearized ends of pMR0107 were assembled using the Gibson Assembly Cloning Kit NEB (Ipswich, MA) according to manufacturer's instructions and subsequently transformed into chemically competent *E. coli* DH5α (Green & Joseph 2001). Primers were ordered from Integrated DNA Technologies (Coralville, IA) unmodified with standard desalting. Primers used are listed in (Supplementary Table S2.1). Primers were designed flanking each extracellular loop of *ompA* to linearize the vector for replacement with a donor sequence from *oprF* in order to construct plasmids pTCA1-pTCA7, based on the Rawling (Rawling et al. 1995) model of OprF secondary structure containing a minimum 15-bp homology to the linearized vector. For replacement of OmpA loop 1 (AA 38-54) pTCA0 was linearized removing (AA 38-54) of *ompA* (Fig. 2.2B). The donor fragment of *oprF* (coding AA 44-50) was amplified with overlapping regions to the linearized vector. Fragments were assembled using Gibson Assembly Cloning Kit NEB (Ipswich, MA) and transformed into DH5α. Loop 2 (coding AA 79-95) and loop 3 (coding AA 125-137) of *ompA* were replaced sequentially with loop 2 (coding AA 77-87) and loop 3 (coding AA 121-130) of *oprF* resulting in pTCA2 and pTCA3 respectively, (Fig. 2.2A). Linearized pTCA0 *ompA* loop 1 (coding AA 38-54) and the donor insert *oprF* loop 5

(coding AA 198-237) were assembled, resulting in pTCA4. Linearized pTCA0 *ompA* loop 2 (coding AA 79-95) and insert *oprF* loop 6 (coding AA 257-275) were assembled to yield pTCA5. Linearized pTCA4 loop 2 (coding AA 79-95) was replaced with *oprF* (coding AA 257-275) to yield pTCA6. Loop 3 (coding AA 125-137) of pTCA6 was linearized and replaced with *oprF* loop 7 (coding AA 310-314), resulting in pTCA7. Constructs based on the Gilleland (Gilleland Jr. et al. 1995) secondary structure model of *oprF* were constructed for loop 5, loop 6, and loops 5&6. Linearized pTCA0 *ompA* loop 1 (AA coding 38-54) or *ompA l*oop 2 (coding AA 79-95) were replaced with *oprF* loop 5 (coding AA 200-217) or loop 6 (coding AA 241-261) to yield constructs pTCA8 and pTCA9 respectively. Loop 2 (coding AA 79-95) of pTCA8 was linearized and replaced with *oprF* loop 6 (coding AA 241-261) and subsequently assembled to yield pTCA10.

Primers for the chromosomal amplification of the *pspA* promoter were designed based on the reported *E. coli* MG1655 sequence from EcoCyc (Keseler et al. 2013). The genomic region containing 240-bp upstream of the *pspA* transcriptional start site was amplified with PspApro_F and PspApro_R (Table S2.1) by PCR with Q5 High Fidelity Polymerase NEB (Ipswich, MA). To construct the pPALacZ1 plasmid, pBAC-LacZ, a gift from Keith Joung (Addgene plasmid # 13422) was linearized with pBAC-LacZ_F, pBAC-LacZ_R, replacing the *lacZ* promoter with the *pspA* promoter, assembled with the Gibson Assembly Cloning Kit NEB (Ipswich, MA) and subsequently transformed into chemically competent *E. coli* DH5α.

All constructs were PCR verified for loop replacements and sequenced by the Cornell Biotechnology Resource Center (Ithaca, NY). Verified constructs pTCA0-

pTCA10 were transformed into electrocompetent *E. coli* JW0940 either individually or with the addition of pBACLacZ1.

Binding Assay

Whole cell enzyme linked immunoassay (ELISA) was used to screen loop constructs for binding of IFN-γ as previously described (Wu et al. 2005). In short, *P. aeruginosa* PAO1, *E. coli* BW25113, and *E. coli* JW0940 harboring plasmids pTCA1-pTCA10 were grown overnight in LB broth containing c*hloramphenicol* (12.5 μg/mL) for vector maintenance at 37°C. Cultures were diluted 1:50 with fresh LB media and grown at 37°C to an OD_{600} of 0.5 to 0.6. Bacteria were harvested and washed twice with PBS. Washed bacteria were fixed in 3.7% paraformaldehyde for 30 minutes and washed twice with PBS. All fixed cultures were adjusted to an OD_{600} of 0.5 with PBS prior to coating Nunc Immobilizer Amino 96 well plates Thermo Fisher Scientific (Waltham, MA). Plates were coated with 100 μL of culture suspension and incubated overnight with gentle rocking at 4°C. Plates were washed with PBST (PBS pH 7.2, 0.05% Tween 20), nonspecific binding sites were subsequently blocked with PBST containing 5% sucrose Malinckrodt Chemicals (Phillipsburg, NJ), and 1X micellar casein Vector Laboratories - SP-5020 (Burlingame, CA) for 1 hour at 37°C. 100 μL of human IFN-γ (1 μg/mL) was added to the microtiter plate and incubated at room temperature for 1 hour. Bound IFN-γ was detected using a Human IFN-γ ELISA kit (ESS0002) from Thermo Scientific (Waltham, MA) with slight modification. Anti-human IFN-γ antibody was diluted 1:500 and incubated for 1 hour at room temperature. Streptavidin labeled horseradish peroxidase (HRP) was diluted 1:400, and incubated at room temperature for 30

minutes. O-phenylamine-diamine was used as the horseradish peroxidase substrate, and the reaction was stopped with 2M H_2SO_4. Absorbance was measured at 450 nm and 550 nm by a BioTek Synergy 4 microplate reader (BioTek, Winooski, VT).

β-galactosidase Activity Assay

Cultures of *E. coli* JW0940, and the parent strain *E. coli* BW25113, were transformed with pPALacZ1, making (BW25113-**R**), and JW0940 harboring pPALacZ1 (JW0940-**R**), pTCA4-pTCA6, pTCA8-pTCA10 were grown in LB media supplemented with appropriate antibiotics and grown overnight at 37°C. Cultures were diluted to an OD_{600} of 0.05 with fresh LB and incubated at 30°C until OD_{600} of 0.2, prior to the addition of an inducer. BW25113-R was tested for response to membrane stress by the addition of 5% or 10% ethanol. Culture response to cytokines IFN-γ or TNF-α was examined at a concentration of 1 nM. The active response range to IFN-γ or TNF-α was examined at concentrations of 0 pM to 1000 pM. All cultures were incubated for 90 minutes as previously optimized, data not shown, at 30°C post induction. Cultures were collected in 200 μL aliquots, OD_{600} was recorded prior to freezing at -80°C to lyse cells. β-galactosidase activity was measured by a kinetic assay (Ramsay et al. 2011). In short, samples were thawed at 37°C, diluted 1:10 with LB media and 10 μL aliquots were dispensed into black polystyrene 96 well plate, Nunc, Thermo Fisher Scientific (Waltham, MA). 100 μL of reaction buffer (PBS pH 7, 2 mg/mL lysozyme, 0.5 mg/mL 4-methylumbelliferyl-β-D-galactopyranoside (dissolved in DMSO)) was dispensed to each well. Immediately following addition of the reaction buffer, fluorescence was monitored by a BioTek Synergy 4 microplate reader BioTek (Winooski, VT) with the following fluorescent parameter; excitation

360 nm, emissions 460 nm, measured every minute for 30 minutes. Relative fluorescence units (RFU) produced per minute for each well was calculated by the linear increase in fluorescence, normalized by OD_{600} of the sample and reported as $RFU/min/OD_{600}$.

Statistics

Experiments were conducted in triplicate with a minimum of three biological replicates sampled for each variable. Error bars, represent 95% confidence intervals.

Results

OprF of *P. aeruginosa* exists as two conformational states with either four or eight extracellular loops (Sugawara et al. 2006; Rawling et al. 1995). The extracellular loop(s) of OprF which bind IFN-γ have not been identified. Therefore, peptides corresponding to six of the eight extracellular loops (excluding loops 4 and 8) of the larger OprF conformation (Fig. 2.2B) were selected for study. Loops 4 and 8 of OprF were excluded because loop 4 of OmpA is not necessary for signal transduction due to extracellular binding of OmpA (Maruvada & Kim 2011). Selected peptides of OprF were used to replace the extracellular loops of OmpA (Fig. 2.2A). The rational design of OmpA/OprF chimera constructs is represented in (Fig. 2.2A), such that loops of OmpA are color coded corresponding to the amino acids they are replaced with from OprF (Fig. 2.2B). Constructs were designed such that loops 1-3 of OmpA were consecutively replaced with loops 1-3 or loops 5-7 of OprF, based on the proposed secondary structure of the large channel conformation (Rawling et al. 1995). Loops were replaced consecutively to determine which extracellular loop(s) of OprF would bind IFN-γ. Further, loops 1 and 2 of OmpA were replaced with loops 5 and 6

of OprF individually and consecutively based on the secondary conformation proposed by Rawling (1995) (pTCA4-pTCA6), and Gilleland (1995) (pTCA8-pTCA10). The two models were compared because they differ in the size of loop 5 which alters the extracellular amino acids of loop 6 of OprF, (Fig. 2.2B). Loop 4 of OmpA was not replaced, since OprF loop 8 elicits an immunological response that may complicate deployment of an engineered probiotic (Ding et al. 2010; Gilleland Jr. et al. 1995). Constructs were transformed into JW0940 (Δ*ompA*) for subsequent examination.

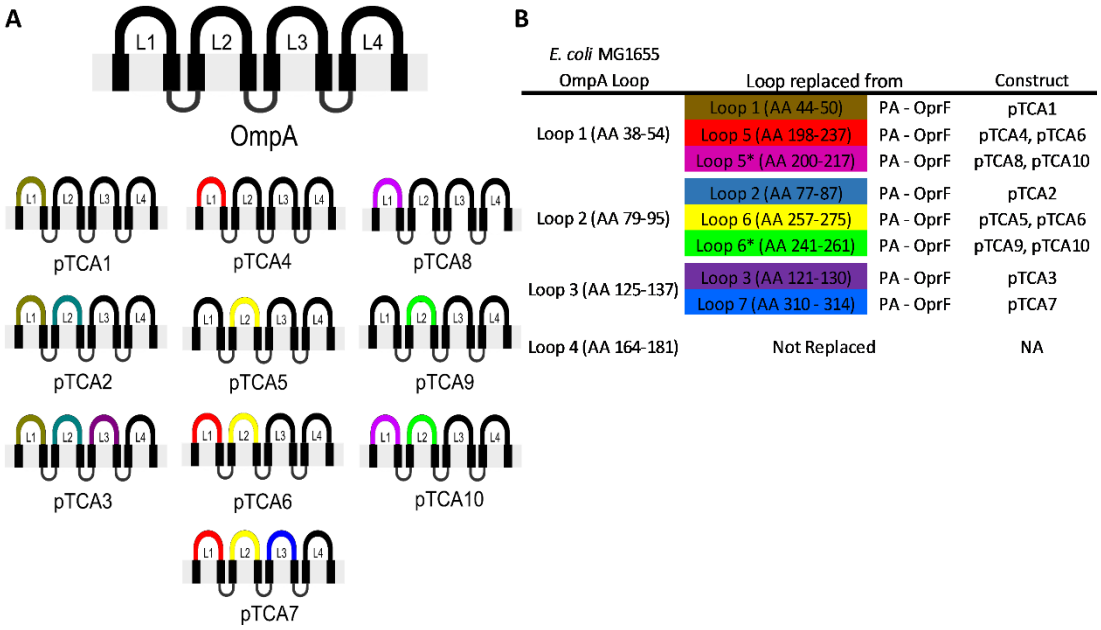

Figure 2.2: Rational design of OmpA/OprF chimeric proteins for the determination of the extracellular peptides of OprF that bind IFN-γ. Color coding of OmpA loops (A) corresponds to the OprF loops they are replaced with in (B). (A) OmpA extracellular loops 1-3 were consecutively replaced with loops 1-3 (pTCA1-pTCA3), or loops 5-7 (pTCA4, pTCA6, pTCA7) of OprF based on the Rawling model. OmpA loop 2 was replaced with OprF loop 6 based on the Rawling model (pTCA5). Loops 1-2 were replaced individually or consecutively with loops 5 and 6 of OprF based on Gilleland model (pTCA8-pTCA10). (B) Amino acids of *E. coli* OmpA loops 1-3 to be replaced with loops 1-3, or 5-7 of *P. aeruginosa* (PA01) OprF, an * indicates peptide fragments based on the secondary structure of Gilleland model.

IFN-γ Binding Determined by Fixed Whole Cell ELISA

There was no significant binding of IFN-γ to strains harboring pTCA1-pTCA3 relative to native OmpA in *E. coli* BW25113 (Fig. S2.1). pTCA4 had significant binding of IFN-γ (Fig. 2.3), the addition of loop 6 (pTCA6) to pTCA4 reduced the capability of loop 5 to bind IFN-γ. Further, constructs pTCA8-pTCA10 based on the Gilleland model (1995) were capable of binding IFN-γ, however, there was no significant difference in binding between constructs. *P. aeruginosa* PAO1 and pTCA4 expressed in JW0940 were capable of binding IFN-γ at a similar concentration (59.5 nM) to the literature (Wu et al. 2005; Ding et al. 2010).

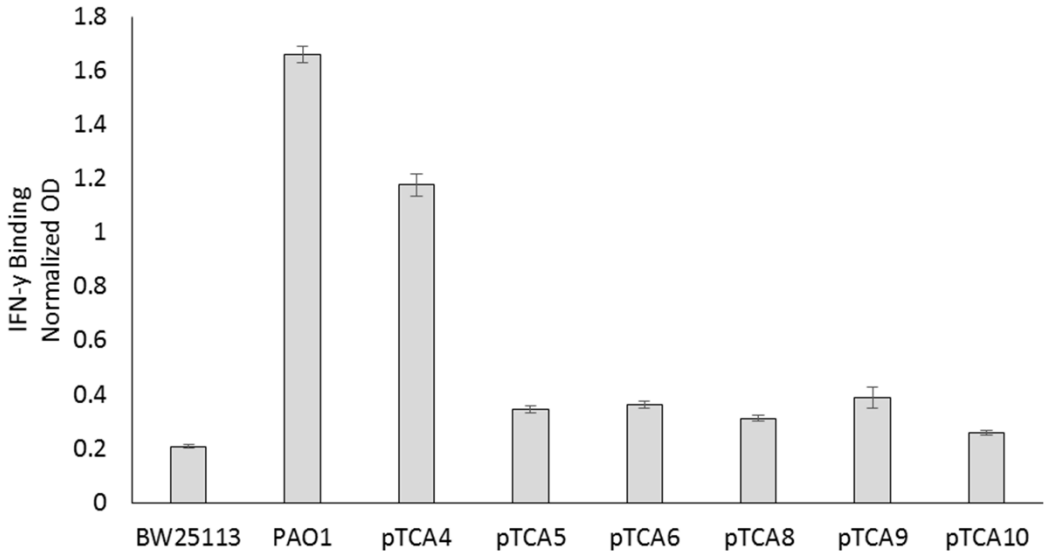

Figure 2.3: Whole cell ELISA for detection of bound IFN-γ. Fixed cells were standardized to an OD_{600} of 0.5 in PBS, and incubated with 59.2 nM of IFN-γ at room temperature. Bound IFN-γ was determined using biotin labeled anti-human IFN-γ antibody, and detected with streptavidin labeled HRP. Absorbance was measured at 450 nm and 550 nm, the mean of three independent experiments (n=5) is represented, error bars, represent 95% CI.

Reporter Testing for Detection of IFN-γ

IFN-γ binding to OmpA/OprF chimeras causing signal transduction to a detectable reporter, is essential for detection of environmental concentrations of IFN-γ. IFN-γ binding to the chimera is transduced by the *pspA* promoter driving expression of *lacZ* (pPALacZ1). Since the *pspA* promoter is typically activated by membrane stress, β-galactosidase activity of pPALacZ1 was characterized by the addition of 5% and 10% ethanol, which has been shown to induce *pspA* expression (Fig. 2.4) (Brissette et al. 1990).

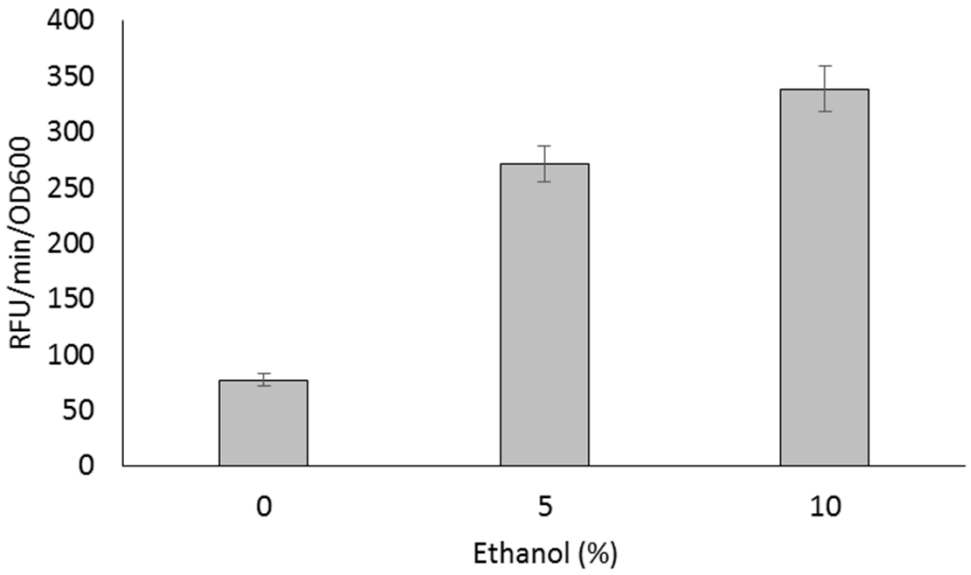

Figure 2.4: *pspA* promoter activity of pPALacZ1 expressed in *E. coli* JW0940 in response to membrane stress induced by 5% and 10% ethanol. Ethanol was added to cultures at an OD_{600} of 0.2 and samples were collected after 90 minutes. β-galactosidase activity of n=8 per treatment were measured as RFU/min, and normalized by OD_{600}. Error bars, represent a 95% CI.

JW0940-R harboring pTCA4-pTCA6, or pTCA8-pTCA10 were tested for an inducible response to 1 nM of IFN-γ or TNF-α, measured by β-galactosidase activity (Fig. 2.5). TNF-α was selected because it acts synergistically with IFN-γ during an inflammatory response and reduces tight junctions between epithelial cells (Li et al. 2008). We wanted to determine if the chimeric constructs could differentiate between TNF-α and IFN-γ during signal transduction. BW25113-R was used as a negative control to establish basal expression levels for pPALacZ1 in a native OmpA background. BW25113-R had no response to IFN-γ or TNF-α above *pspA* basal expression (Fig. 2.5). JW0940-R harboring pTCA4 (Fig. 2.5A) or pTCA9 (Fig. 2.5B) showed selective response to IFN-γ. However, JW0940-R harboring pTCA6, (Fig. 2.5A), or pTCA10 (Fig. 2.5B) harboring double loop replacements, were unable to differentiate between IFN-γ and TNF-α, though both had elevated activity. Based on these results, pTCA4, pTCA6, pTCA9, and pTCA10 were selected to determine the active range of IFN-γ and TNF-α induced β-galactosidase activity.

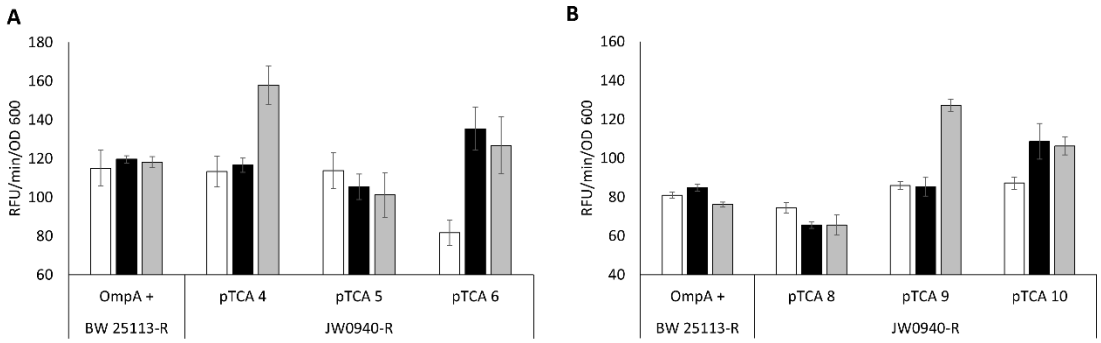

Figure 2.5: β-galactosidase activity of pPALacZ1 upon the addition of: no inducer (white), 1 nM TNF-α (Black), or 1 nM IFN-γ (grey), to BW25113-R (native OmpA) or JW0940-R harboring pTCA4-pTCA6 (A), or pTCA8-pTCA10 (B). β-galactosidase expression was measured as RFU/min for n=8 of each treatment, and normalized by OD_{600}. Error bars, represent a 95% CI.

Active Range of IFN-γ Binding

The threshold concentration at which pPALacZ1 produces β-galactosidase in response to IFN-γ binding, is depicted in (Fig. 2.6), pTCA4 (A), pTCA6 (B), pTCA9 (C), and pTCA10 (D). Cultures were induced with IFN-γ or TNF-α at concentrations of 0 to 1000 pM, and sampled after 90 minutes of incubation (Fig. 2.6). pTCA4, was consistently induced by as little as 300 pM of IFN-γ, whereas, there was no change in β-galactosidase activity for TNF-α (Fig. 2.6A). However, with the addition of loop 6, (pTCA6) TNF-α induced β-galactosidase activity and increased the noise seen in response to IFN-γ (Fig. 2.6B). Constructs pTCA9 and pTCA10, (Figs. 2.6 C & D) respectively, required higher concentrations of IFN-γ or TNF-α, to induce a detectable response. pTCA9, (Fig. 2.6C), produced a response to 900 pM of IFN-γ, whereas, pTCA10, (Fig. 2.6D), containing both loops 5 and 6 had a response to 800 pM of TNF-α and 900 pM of IFN-γ. The replacement of loops 1 and 2 of OmpA with loops 5 and 6 of OprF of either the Rawlings (1995) or Gilleland (1995) models elicits a response to both inflammatory cytokines IFN-γ and TNF-α. However, pTCA4 (which replaces loop 1 of OmpA with loop 5 of OprF from the Rawling model (1995)) was significantly more sensitive and specific to IFN-γ.

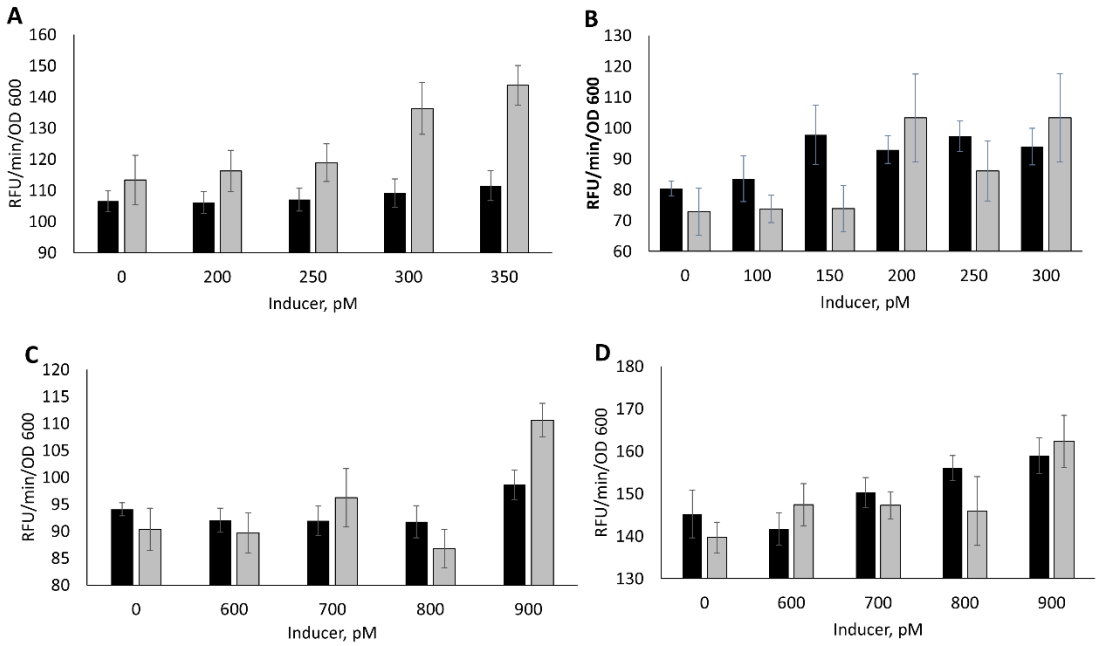

Figure 2.6: Active range of (A) pTCA4, (B) pTCA6, (C) pTCA9, (D) pTCA10, to TNF-α (black) and IFN-γ (grey) over concentrations of 0 pM to 900 pM. β-galactosidase activity was measured in RFU/min for n=8 per treatment, and normalized by OD_{600}. Error bars, represent a CI of 95%.

Discussion

Engineering probiotic bacteria capable of sensing disease biomarkers in the lumen and responding as a therapeutic for the treatment of disease has been the subject of several reviews and studies (Aurand et al. 2012; Goh et al. 2012). The epithelial cells of the intestine act as a defensive barrier preventing the translocation of antigens into the host, and permeation of host biomarkers into the intestinal lumen. However, the protection provided by the intestinal epithelium is disrupted in inflammatory bowel disease (IBD), including ulcerative colitis (UC) and Crohn's disease (CD) as a result of inflammation and epithelial injury (Neurath 2014). Genetic susceptibility and environmental cues initiate disruption of the intestinal epithelium, allowing translocation of antigens (microbes) which induce the production of inflammatory cytokines by immune cells. Failure to mediate an inflammatory response leads to chronic inflammation of the intestine and mucosal tissue damage (Hatoum et al. 2006). Sites of chronic inflammation have increased local concentrations of IFN-γ and TNF-α in addition to a permeable intestinal barrier that permits the release of inflammatory cytokines from the lamina propria into the lumen of the intestine (Murch et al. 1993; Barry et al. 2011). Here we report a novel bacteria based detection system for the cytokines IFN-γ and TNF-α. The system was constructed in such a way that binding of IFN-γ or TNF-α to an OmpA/OprF chimeric protein induces expression of the *pspA* controlled reporter.

To create the OmpA/OprF chimera, we tested which peptide fragments from amino acids 44-342 of OprF were capable of binding IFN-γ. Based on previous studies (Wu et al. 2005; Ding et al. 2010), we expected that amino acids 190-342

would have some binding capability. There are two secondary structural models proposed for the single domain conformation of OprF (Gilleland Jr. et al. 1995; Rawling et al. 1995). Extracellular loops used in the design of the chimeric constructs were based on the single domain conformation of OprF. We identified that loops 1-3 and loop 7 of OprF had no significant IFN-γ binding capability (Fig. S2.1). Further, loop 7 of OprF was an undesirable candidate for use in a therapeutic, because it elicited an immunogenic response and is part of the OprF fragment used as an OprF/OprI vaccine for *P. aeruginosa* (Ding et al. 2010; Gilleland Jr. et al. 1995; Hughes et al. 1992). We determined that constructs expressing loop 5 and loop 6, individually (pTCA4, pTCA9) or in combination (pTCA6 and pTCA10) were capable of binding IFN-γ (Fig. 2.3).

The binding site of the human IFN-γ receptor 1 (hIFNGR1) resembles a ball, the ball is formed by amino acids Tyr49, Trp82 and Glu101 of hIFNGR1, which sits in a corresponding hole on IFN-γ during binding (Randal & Kossiakoff 2001). Further, Ectromelia virus (ECTV), the causative agent of mousepox, expresses an IFN-γ binding protein (IFN-γ^{BP}) which exhibits relaxed species specificity for IFN-γ, capable of binding human, murine and rabbit IFN-γ (Mossman et al. 1995). ECTV IFN-γ^{BP} and hIFNGR1 share approximately 20% identity, the receptor binding site of the IFN-γ^{BP} mimics the hIFNGR1 site, furthermore, the IFN-γ^{BP} binds the C-terminus tail of IFN-γ (Nuara et al. 2008; Walter et al. 1995). The proposed secondary structure of pTCA8 (Fig. 2.7A), and pTCA4 (Fig. 2.7B) share 42% identity to the ECTV IFN-γ^{BP} (yellow amino acids), which are adjacent to the IFN-γ receptor binding site. However, pTCA4 had a significantly higher binding capacity for IFN-γ (Fig. 2.3),

possibly because it contains amino acids that share 56% identity to hIFNGR1 (Fig. 2.7B) (shaded in blue), which flank the hIFNGR1 binding site.

Secondly, we propose that IFN-γ binding is partially facilitated by the net charge of the replaced extracellular loops. pTCA4 (loop 5) has a net charge of -7.2, and pTCA9 (loop 6) has a net charge of -5, facilitating interaction of the extracellular loop with the C-terminal tail of IFN-γ (net charge of +2). Further, the ECTV IFN-γ^{BP} was shown to form extensive interactions with the C-terminal tail of IFN-γ (Nuara et al. 2007). Nevertheless, pTCA4 had a greater binding capacity for IFN-γ than pTCA9 (Fig. 2.3) and was capable of induction of the *pspA* reporter upon IFN-γ binding (Fig. 2.5A). These differences could be a result of the larger loop structure of pTCA4 (Fig. 2.7B) due to increased protein flexibility, allowing for greater changes in conformation and increased affinity for a target (Davis & Teague 1999).

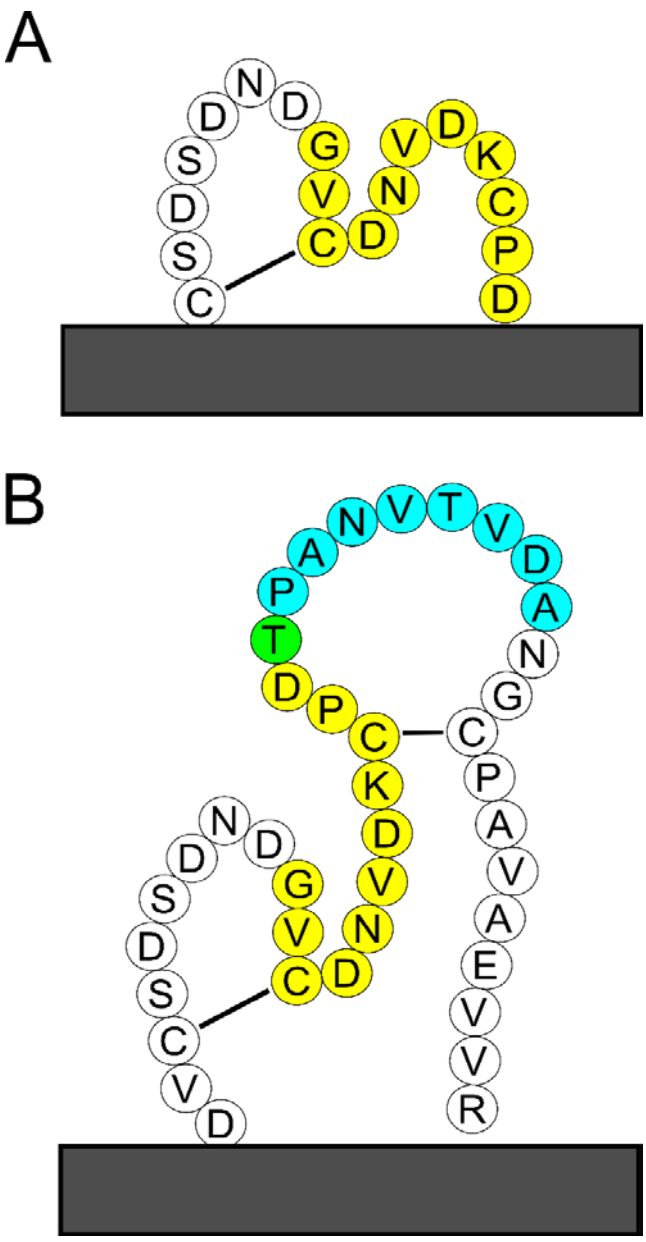

Figure 7: Proposed secondary structure of OprF, **(A)** loop 5 (pTCA8) proposed by Gilleland model (amino acids 200-217), **(B)** loop 5 (pTCA4) Rawling model (amino acids 198-237). Amino acids colored yellow share 42% identify to the amino acids adjacent to the ECTV IFN-γ^{BP} binding site for IFN-γ, blue amino acids share 56% identity to the hINFGR1 binding site of IFN-γ and the amino acid in green was part of both identified sequences.

JW0940-R harboring pTCA9 loop 6 of the Gilleland model (1995) was capable of binding IFN-γ and subsequently transduce cell signaling (Fig. 2.5B). pTCA9 shares 42% sequence identity with hIFNGR1 amino acids 92-103, which are contained in the IFN-γ binding site (Randal & Kossiakoff 2001). The specificity of pTCA4 and pTCA9 for IFN-γ detection makes them exceptional candidates for the detection of inflammation in the gut. Nevertheless, the active dose of IFN-γ for pTCA4 is 300 pM (Fig. 2.6A), and pTCA9 is 900 pM (Fig. 2.6B), making pTCA4 the optimal candidate for IFN-γ detection. Furthermore, constructs pTCA6 and pTCA10 responded to TNF-α (Fig. 2.5), and were capable of detecting TNF-α at concentrations of 150 pM, (Fig. 2.6B) and 800 pM (Fig. 2.6D), respectively. Concentrations of TNF-α found in stool samples of relapsed IBD patients were 15.9-343.8 pM (Braegger et al. 1992), within the detection limits presented here. The capacity to detect IFN-γ with pTCA4 and TNF-α with pTCA6 allows for the opportunity to develop independent bacterial sensors for the detection of inflammatory cytokines that could work simultaneously to identify sites of inflammation.

In conclusion, we have engineered *E. coli* capable of detecting the inflammatory cytokines IFN-γ and TNF-α at an active concentration of 300 pM and 150 pM, respectively. Detection occurs by means of an OmpA/OprF chimeric protein that induces a *pspA* reporter upon cytokine binding. Further, we identified, loop 5 and loop 6 of the single domain conformational Rawling model (1995) and Gilleland model (1995), respectively, are capable of binding IFN-γ. Loops 5 and 6 in combination, were capable of interacting with TNF-α. The OmpA/OprF chimera developed in this study, pTCA4 in a probiotic strain, would allow the development of

therapeutics capable of detecting sites of inflammation within the intestine. Induction of the *pspA* promoter in response to IFN-γ and TNF-α binding allows for the development of a therapeutic capable of identifying regions of inflammation, and responding with proper treatment to reduce inflammation.

References

Aurand, T.C., Russell, M.S. & March, J.C., 2012. Synthetic signaling networks for therapeutic applications. *Current opinion in biotechnology*, 23(5), pp.773–779. Available at: http://www.ncbi.nlm.nih.gov/pubmed/22285057 [Accessed December 23, 2012].

Baba, T. et al., 2006. Construction of Escherichia coli K-12 in-frame, single-gene knockout mutants: the Keio collection. *Molecular systems biology*, 2(1), p.2006.0008. Available at: http://msb.embopress.org/content/2/1/2006.0008.abstract.

Barry, S. et al., 2011. Cells, cytokines and inflammatory bowel disease: a clinical perspective. *Expert Review of Gastroenterology & Hepatology*, 5, pp.703–716. Available at: http://go.galegroup.com/ps/i.do?id=GALE%7CA283017505&v=2.1&u=nysl_sc_cornl&it=r&p=AONE&sw=w&asid=6738714ee43696c696df93011dc0bc4a.

Braegger, C.P. et al., 1992. Tumour necrosis factor alpha in stool as a marker of intestinal inflammation. *The Lancet*, 339(8785), pp.89–91. Available at: http://www.sciencedirect.com/science/article/pii/014067369290999J.

Brissette, J.L. et al., 1990. Phage shock protein, a stress protein of Escherichia coli. *Proceedings of the National Academy of Sciences of the United States of America*, 87(3), pp.862–866. Available at: http://www.pnas.org/content/87/3/862.abstract.

Clarke, M.B. et al., 2006. The QseC sensor kinase: A bacterial adrenergic receptor.

Proceedings of the National Academy of Sciences , 103 (27), pp.10420–10425. Available at: http://www.pnas.org/content/103/27/10420.abstract.

Davis, A.M. & Teague, S.J., 1999. Hydrogen Bonding, Hydrophobic Interactions, and Failure of the Rigid Receptor Hypothesis. *Angewandte Chemie International Edition*, 38(6), pp.736–749. Available at: http://dx.doi.org/10.1002/(SICI)1521-3773(19990315)38:6<736::AID-ANIE736>3.0.CO.

Ding, B., von Specht, B.-U. & Li, Y., 2010. OprF/I-vaccinated sera inhibit binding of human interferon-gamma to Pseudomonas aeruginosa. *Vaccine*, 28(25), pp.4119–4122. Available at: http://www.sciencedirect.com/science/article/B6TD4-4YYF2MG-6/2/dea51d95d4b4181bc18eeaa0d7bde91e.

Duan, F., Curtis, K.L. & March, J.C., 2008. Secretion of Insulinotropic Proteins by Commensal Bacteria: Rewiring the Gut To Treat Diabetes. *Applied and Environmental Microbiology* , 74 (23), pp.7437–7438. Available at: http://aem.asm.org/content/74/23/7437.abstract.

Duan, F.F., Liu, J.H. & March, J.C., 2015. Engineered Commensal Bacteria Reprogram Intestinal Cells Into Glucose-Responsive Insulin-Secreting Cells for the Treatment of Diabetes. *Diabetes*, 64(5), pp.1794–1803. Available at: http://diabetes.diabetesjournals.org/lookup/doi/10.2337/db14-0635.

Gibson, D.G. et al., 2009. Enzymatic assembly of DNA molecules up to several hundred kilobases. *Nat Meth*, 6(5), pp.343–345. Available at: http://dx.doi.org/10.1038/nmeth.1318.

Gilleland Jr., H. et al., 1995. Use of synthetic peptides to identify surface-exposed,

linear B-cell epitopes within outer membrane protein F of Pseudomonas aeruginosa. *Current Microbiology*, 31(5), pp.279–286. Available at: http://dx.doi.org/10.1007/BF00314580.

Goh, Y.-L., He, H. & March, J.C., 2012. Engineering commensal bacteria for prophylaxis against infection. *Current Opinion in Biotechnology*, 23(6), pp.924–930. Available at: http://www.sciencedirect.com/science/article/pii/S0958166912000511.

Green, M.R. & Joseph, S., 2001. Molecular cloning: a laboratory manual.

Hatoum, O.A., Heidemann, J. & Binion, D.G., 2006. The Intestinal Microvasculature as a Therapeutic Target in Inflammatory Bowel Disease. *Annals of the New York Academy of Sciences*, 1072(1), pp.78–97. Available at: http://dx.doi.org/10.1196/annals.1326.003.

Hughes, D.T. & Sperandio, V., 2008. Inter-kingdom signalling: communication between bacteria and their hosts. *Nat Rev Micro*, 6(2), pp.111–120. Available at: http://dx.doi.org/10.1038/nrmicro1836.

Hughes, E.E., Gilleland, L.B. & Gilleland, H.E., 1992. Synthetic peptides representing epitopes of outer membrane protein F of Pseudomonas aeruginosa that elicit antibodies reactive with whole cells of heterologous immunotype strains of P. aeruginosa. *Infection and Immunity* , 60 (9), pp.3497–3503. Available at: http://iai.asm.org/content/60/9/3497.abstract.

Joly, N. et al., 2010. Managing membrane stress: the phage shock protein (Psp) response, from molecular mechanisms to physiology. *FEMS Microbiology*

Reviews, 34(5), pp.797–827. Available at: http://dx.doi.org/10.1111/j.1574-6976.2010.00240.x.

Keseler, I.M. et al., 2013. EcoCyc: fusing model organism databases with systems biology. *Nucleic Acids Research* , 41 (D1), pp.D605–D612. Available at: http://nar.oxfordjournals.org/content/41/D1/D605.abstract.

Khalid, S. et al., 2006. Modeling and simulations of a bacterial outer membrane protein: OprF from Pseudomonas aeruginosa. *Proteins: Structure, Function, and Bioinformatics*, 63(1), pp.6–15. Available at: http://dx.doi.org/10.1002/prot.20845.

Koebnik, R., 1999. Structural and functional roles of the surface-exposed loops of the beta-barrel membrane protein OmpA from Escherichia coli. *J. Bacteriol.*, 181(12), pp.3688–3694. Available at: http://jb.asm.org/cgi/content/abstract/181/12/3688.

Koebnik, R., Locher, K.P. & Van Gelder, P., 2000. Structure and function of bacterial outer membrane proteins: barrels in a nutshell. *Molecular Microbiology*, 37(2), pp.239–253. Available at: http://dx.doi.org/10.1046/j.1365-2958.2000.01983.x.

Laughlin, R.S. et al., 2000. The Key Role of Pseudomonas aeruginosa PA-I Lectin on Experimental Gut-Derived Sepsis. *Annals of Surgery*, 232(1), pp.133–142. Available at: http://www.ncbi.nlm.nih.gov/pmc/articles/PMC1421122/.

Li, Q. et al., 2008. Interferon-γ and tumor necrosis factor-α disrupt epithelial barrier function by altering lipid composition in membrane microdomains of tight junction. *Clinical Immunology*, 126(1), pp.67–80. Available at:

http://www.sciencedirect.com/science/article/pii/S1521661607013307.

Maruvada, R. & Kim, K.S., 2011. Extracellular Loops of the Eschericia coli Outer Membrane Protein A Contribute to the Pathogenesis of Meningitis. *The Journal of Infectious Diseases*, 203(1), pp.131–140. Available at: http://www.ncbi.nlm.nih.gov/pmc/articles/PMC3086434/.

Model, P., Jovanovic, G. & Dworkin, J., 1997. The Escherichia coli phage-shock-protein (psp) operon. *Molecular Microbiology*, 24(2), pp.255–261. Available at: http://dx.doi.org/10.1046/j.1365-2958.1997.3481712.x.

Mossman, K. et al., 1995. Species Specificity of Ectromelia Virus and Vaccinia Virus Interferon-γ Binding Proteins. *Virology*, 208(2), pp.762–769. Available at: http://www.sciencedirect.com/science/article/pii/S0042682285712081.

Murch, S.H. et al., 1993. Location of tumour necrosis factor alpha by immunohistochemistry in chronic inflammatory bowel disease. *Gut*, 34(12), pp.1705–1709. Available at: http://www.ncbi.nlm.nih.gov/pmc/articles/PMC1374467/.

Neurath, M.F., 2014. Cytokines in inflammatory bowel disease. *Nat Rev Immunol*, 14(5), pp.329–342. Available at: http://dx.doi.org/10.1038/nri3661.

Nuara, A.A. et al., 2008. Structure and mechanism of IFN-Î³ antagonism by an orthopoxvirus IFN-Î³-binding protein. *Proceedings of the National Academy of Sciences*, 105(6), pp.1861–1866. Available at: http://www.pnas.org/content/105/6/1861.abstract.

Nuara, A.A., Buller, R.M.L. & Bai, H., 2007. Identification of residues in the

ectromelia virus gamma interferon-binding protein involved in expanded species specificity. *J Gen Virol*, 88(1), pp.51–60. Available at: http://vir.sgmjournals.org/cgi/content/abstract/88/1/51.

Pautsch, A. & Schulz, G.E., 2000. High-resolution structure of the OmpA membrane domain. *Journal of Molecular Biology*, 298(2), pp.273–282. Available at: http://www.sciencedirect.com/science/article/pii/S0022283600936714.

Ramsay, J.P. et al., 2011. A quorum-sensing molecule acts as a morphogen controlling gas vesicle organelle biogenesis and adaptive flotation in an enterobacterium. *Proceedings of the National Academy of Sciences* , 108 (36), pp.14932–14937. Available at: http://www.pnas.org/content/108/36/14932.abstract.

Randal, M. & Kossiakoff, A.A., 2001. The Structure and Activity of a Monomeric Interferon-γ:α-Chain Receptor Signaling Complex. *Structure*, 9(2), pp.155–163. Available at: http://www.sciencedirect.com/science/article/pii/S0969212601005676.

Rawling, E.G., Martin, N.L. & Hancock, R.E., 1995. Epitope mapping of the Pseudomonas aeruginosa major outer membrane porin protein OprF. *Infect. Immun.*, 63(1), pp.38–42. Available at: http://iai.asm.org/cgi/content/abstract/63/1/38.

Sperandio, V. et al., 2003. Bacteria–host communication: The language of hormones. *Proceedings of the National Academy of Sciences* , 100 (15), pp.8951–8956. Available at: http://www.pnas.org/content/100/15/8951.abstract.

Sugawara, E. et al., 2006. Pseudomonas aeruginosa Porin OprF Exists in Two

Different Conformations. *Journal of Biological Chemistry*, 281(24), pp.16220–16229. Available at: http://www.jbc.org/content/281/24/16220.abstract.

Verhoeven, G.S. et al., 2009. Differential Bacterial Surface Display of Peptides by the Transmembrane Domain of OmpA. *PLoS ONE*, 4(8), p.e6739. Available at: http://dx.doi.org/10.1371/journal.pone.0006739.

Walter, M.R. et al., 1995. Crystal structure of a complex between interferon-[gamma] and its soluble high-affinity receptor. *Nature*, 376(6537), pp.230–235. Available at: http://dx.doi.org/10.1038/376230a0.

Weiner, L., Brissette, J.L. & Model, P., 1991. Stress-induced expression of the Escherichia coli phage shock protein operon is dependent on sigma 54 and modulated by positive and negative feedback mechanisms. *Genes & Development* , 5 (10), pp.1912–1923. Available at: http://genesdev.cshlp.org/content/5/10/1912.abstract.

Wu, L. et al., 2005. Recognition of Host Immune Activation by Pseudomonas aeruginosa. *Science*, 309(5735), pp.774–777. Available at: http://www.sciencemag.org/content/309/5735/774.abstract.

CHAPTER THREE

In vitro Detection of Interferon-γ and Tumor Necrosis Factor-α by a Whole Cell Synthetic Detection System*

* Thomas Christopher Aurand, Matthew S. Russell, Cait M. Costello, John C. March

Abstract

Inflammatory bowel disease (IBD) is characterized as chronic inflammation of the gastrointestinal tract in which cytokines play a direct role in the pathogenesis of the disease. The incidence of IBD has been increasing worldwide as countries become industrialized and currently affects 1.5 million Americans and 2.2 million Europeans (Molodecky et al. 2012). A non-invasive and inexpensive means to assay inflammation markers by a whole cell bacterial sensor was examined. Here, we showed that basolateral application of interferon-γ (IFN-γ) and tumor necrosis factor α (TNF-α) induced Caco-2 barrier dysfunction *in vitro*. Caco-2 cells were grown on Transwell® inserts to simulate the intestinal epithelium, cytokines were applied to the basolateral chamber (lamina propria), inducing barrier dysfunctions, permitting permeation of the cytokines into the apical chamber (intestinal lumen). Further, a bacteria based assay demonstrated IFN-γ and TNF-α could be detected at a threshold concentration of 14 pM and 15.1 pM respectively *in vitro*. The bacterial based assay had an accuracy of 95% to detect cytokines above the established threshold concentration.

Introduction

The intestinal epithelium consists of a single layer of cells that act as a barrier under normal healthy conditions. This barrier prevents luminal bacteria and noxious agents from permeating into the host while permitting the uptake of nutrients and selectively releasing host immune modulators into the luminal environment (Rescigno 2011; Groschwitz & Hogan 2009). Sealing of this barrier is established by the formation of tight junctions between epithelial cells. At the juncture there are two

types of pores governing paracellular transport of molecules; restrictive pores which permit small molecules (water, ions, mannitol), and non-restrictive pores that permit large molecules to pass (dextran and graded polyethylene polymers (PEG)) (Watson et al. 2001). Further, tight junctions selectively prevent the translocation of antigens and bacteria from crossing the barrier.

However, under conditions of inflammation the intestinal barrier is dysfunctional, permitting permeation of inflammatory agonists. The intestinal barrier becomes leaky in inflammation based disease such as inflammatory bowel disease, IBD (Crohn's disease and ulcerative colitis), irritable bowel disease (IBS), and bacterial infection (Al-Sadi et al. 2009). IBD is defined as chronic inflammation of the intestinal mucosa induced by genetic predisposition and environmental factors (Hanauer 2006). Chronic inflammation in IBD is the result of an upregulated immune response to an agonist that does not resolve once the agonist has been removed. Increased pro-inflammatory cytokines: interferon-γ (IFN-γ), tumor necrosis factor-α (TNF-α), interleukin-1β (IL-1β) and IL-12 present in the submucosa, lead to further increases in intestinal epithelial permeability allowing for the inflammatory cycle to persist (Hanauer 2006; Al-Sadi et al. 2009; MacDonald et al. 1990).

The pro-inflammatory cytokines IFN-γ and TNF-α have been implicated in the pathogenesis of IBD (MacDonald et al. 1990). IFN-γ and TNF-α have been shown to increase intestinal permeability independently and synergistically (Ma et al. 2004; Madara & Stafford 1989; Fish et al. 1999). Some *in vitro* models, showed a maximum reduction in transepithelial electrical resistance (TEER), a method for determining paracellular permeability, after 48 hours of basolateral exposure of intestinal epithelial

monolayers to IFN-γ or TNF-α (Wang et al. 2005). Further, Watson *et al* (2005) demonstrated that IFN-γ induced a selective increase in paracellular permeability for larger molecules (7.4 – 23 Å). The selective increase in permeability of larger molecules to translocate across the epithelial barrier may also permit the release of inflammatory cytokines into the intestinal lumen. Measuring the presence of abnormal concentrations of cytokines in the lumen could be used for detection of the onset and relapse of IBD. One such study, by Braegger *et al* (1992) demonstrated that TNF-α could be detected in the stool of patients with Crohn's disease and ulcerative colitis at concentrations of 57.1 pM and a range of 15.8-343.8 pM respectively. However, the presence of IFN-γ has not been detectable in stool samples as of yet, which may be the result of disease progression at the time of sampling because IFN-γ is involved in the early stages of IBD (Spencer et al. 2002). This suggest that localized rapid detection systems which can monitor for cytokines in real time are needed, for example, bacterial based bioreporters (Carty et al. 2000; Aurand et al. 2012).

The advantage of a biological bioreporter is it can be tailored to respond to localized environmental cues, and rapidly detect early warning signs of inflammation at the site, prior to the emergence of symptoms to the host. Eventually, bacterial based bioreporters could be developed to deliver localized treatment as needed, rather than administration of a therapeutic compound by means of injection or surgery. For example, previous work has shown potential for the treatment of IBD through the application of an engineered strain of *Lactococcus lactis* which constitutively produced IL-10 to improve barrier function, a 50% reduction in dextran-induced

colitis in mice was observed (Steidler et al. 2000).

Previously we developed an *E. coli* based bioreporter system capable of detecting IFN-γ and TNF-α at concentrations of 300 pM and 150 pM respectively (Aurand & March 2015). The whole cell bioreporter consisted of a chimeric protein of OmpA and OprF located on the outer membrane of *E. coli*. Binding of IFN-γ or TNF-α to the engineered receptor drives production of β-galactosidase under the control of the phage shock protein A (*pspA*) promoter.

For this investigation, we wanted to examine if the previously developed whole cell bioreporter was capable of detecting luminal IFN-γ and TNF-α. First, we tested if basolateral exposure of Caco-2 monolayers to IFN-γ and TNF-α lead to intestinal epithelial barrier dysfunction, thus permitting the paracellular transport of cytokines. Secondly, the minimum detectable concentration of cytokines which permeated into the "lumen" or apical chamber was determined for the whole cell bioreporter.

Materials and Methods

The bacterial bioreporter used in this study consists of *E. coli* JW0940 (*ΔompA::kan*) (Baba et al. 2006) harboring the reporter construct pPALacZ1, *pspA* promoter driving expression of *lacZ*, referred to as JW0940-R and pTCA4 or pTCA6 expressing an OmpA/OprF chimeric fusion capable of binding IFN-γ or TNF-α (Aurand & March 2015). Cytokines used in this study were recombinant human IFN-γ and recombinant human TNF-α R&D Life Sciences (Menomonie, WI).

Cell Culture

Caco-2 cells originating from a human colorectal carcinoma were obtained

from ATCC (Manassas, VA) passage 18-25, were expanded and maintained in media [DMEM with 10% Fetal Bovine Serum (FBS), 1X anti-anti] Invitrogen (Long Island, NY). Cells were maintained at 37°C in a humidified incubator with 5% CO_2, with regular passage 1-2 times per week and medium was changed every 2 days. Caco-2 cells were seeded onto polyester 24 mm Transwell® membrane inserts from Corning-Costar (Acton, MA) at a concentration of 5 X 10^4 cells/mL and grown to confluence and a TEER of over 500 ohms*cm^2. Medium was replaced every 2 days in the basolateral and apical chambers. Antibiotics were removed from culture media prior to cytokine application.

Transepithelial Electrical Resistance (TEER)

TEER values of Caco-2 monolayers were measured pre and post cytokine treatment to determine changes in paracellular permeability of monolayers (Watson et al. 2005). Medium was aspirated from the inserts, replaced with fresh DMEM and incubated at 37°C for 15 minutes. TEER was measured with an EVOM2 epithelial voltohmmeter with a STX3 electrode World Precision Instruments (Sarasota, FL). Electrodes were placed in the apical and basolateral chambers, resistance was measured across barrier, corrected for surface area and expressed as Ω*cm^2. To examine the dose effects of IFN-γ and TNF-α on TEER, basolateral application of 1.44-5.75 nM of IFN-γ and TNF-α alone or in combination was applied to Caco-2 monolayers for 48 hours. An additional dose of IFN-γ or TNF-α was added 3 hours prior to post treatment measurement of monolayer TEER. Medium was removed from the apical and basolateral chamber after TEER values were obtained for ELISA quantification and bacterial detection. Three wells per treatment were tested and

experiments were repeated in triplicate.

Bacterial Detection

Cultures of JW0940-**R** harboring pTCA4 or pTCA6 were grown overnight at 37°C in LB media supplemented with 12.5 μg/mL of chloramphenicol and 10 μg/mL of tetracycline. Bacterial detection of cytokines was performed both indirectly and directly. In the indirect method, cultures of bacteria were diluted to an OD_{600} of 0.05 with fresh LB and incubated at 30°C until an OD_{600} of 0.2 was obtained. Apical chamber supernatant was added to cultures at a 1:4 ratio and incubated at 30°C for 90 minutes. For the direct method, bacterial cultures were added to the apical chamber of the treated Caco-2 monolayers to an OD_{600} of 0.2 and incubated for 60 minutes at 30°C. Incubation times and temperatures were previously optimized, data not shown. In both methods, a 100 μL aliquot of each culture was collected, OD_{600} was measured and samples were frozen at -80°C. β-galactosidase activity was measured by a kinetic assay as previously described (Ramsay et al. 2011; Aurand & March 2015). Briefly, apical culture aliquots were thawed, diluted 1:10 with LB media, and 10 μL aliquots were dispensed into a black polystyrene 96 well plate Thermo Scientific Nunc (Waltham, MA) 100 μL of reaction buffer (PBS pH 7, 2 mg/mL lysozyme, 0.5 mg/mL 4-methylumbelliferyl-β-D-galactopyranoside (dissolved in DMSO)) was dispensed to each well. Fluorescence was measured every minute for 30 minutes with the following fluorescent parameters: excitation 360 nm, and emissions 460nm by a BioTek Synergy 4 microplate reader BioTek (Winooski, VT). Relative fluorescence units, (RFU) produced per minute for each well were calculated by the linear increase in fluorescence, normalized by the OD_{600} of the sample and reported as

RFU/min/OD_{600}.

Enzyme Linked Immunoassay (ELISA)

Quantification of IFN-γ and TNF-α in the basolateral and apical chamber supernatant of the Transwell® inserts was conducted using ELISA. IFN-γ was quantified using the Human IFN-γ ELISA Reagent kit Thermo Scientific (Waltham, MA). With slight modification, blocking solution was substituted with 1X micellar casein (Vector Laboratories - SP-5020, Burlingame, CA). Apical samples were diluted 1:5 with PBS. TNF-α concentrations were quantified with the Human TNF-α ELISA development kit Peprotech (Rocky Hill, NJ). Apical samples were diluted 1:2 with PBS. Absorbance was measured at 450 nm and 550 nm by a BioTek Synergy 4 microplate reader (BioTek, Winooski, VT).

Apparent permeability coefficient was calculated for transport of IFN-γ and TNF-α from the basolateral to apical chamber using the following equation:

$$P_{app} = V_r \, x \, (dC) \, / \, (\mathrm{dt}) \, \mathrm{x} \, 1/\mathrm{AC_o}$$

such that V_r is the volume of the apical chamber, dC/dt is the concentration of the cytokine in the apical chamber over time, A is the membrane surface area and C_o is the initial concentration of the basolateral chamber (Artursson & Karlsson 1991).

Statistics

Experiments were conducted in triplicate with a minimum of three biological replicates sampled for each variable. Error bars represent 95% confidence intervals (CI). A fitted line plot was constructed using Minitab® to obtain the response curve of reporter constructs, pTCA4 or pTCA6 to specific IFN-γ and TNF-α concentrations (pM) measured by ELISA. Prediction intervals (PI) of 90% and Confidence intervals

(CI) of 95% were applied to the model. Prediction intervals of 90% were used for the determination of positive cytokine detection threshold concentration (compared to 0 pM) with a 5% chance of type one error.

Results and Discussion

The purpose of this study was to determine if induction of a "leaky" epithelial barrier by the inflammatory mediators IFN-γ and TNF-α would permit the translocation of basolateraly applied cytokines to cross an epithelial monolayer into the "lumen" or apical chamber. Further, we examined the effectiveness of a previously characterized whole cell bioreporter to directly and indirectly detect IFN-γ and TNF-α in an *in vitro* system.

Effect of IFN-γ and TNF-α on Caco-2 Monolayer Barrier Integrity

Basolateral application of IFN-γ and TNF-α alone or in combination for 48 hours produced a reduction in TEER of the Caco-2 monolayers (Fig. 3.1A). Individual application of IFN-γ or TNF-α resulted in a 20% reduction of TEER, however, in combination a 30% reduction in TEER was observed. A reduction in TEER is correlated to disruption of the tight junctions, permitting paracellular permeability and bidirectional flux of molecules across the barrier (Cox et al. 2001). Therefore, we examined the cytokine concentrations in the apical chamber (Fig 3.1 B & C). Cytokine transport increased with greater concentrations of IFN-γ and TNF-α in the basolateral chamber. Previous work by Watson *et al* (2005), showed that basolateral application of IFN-γ increased paracellular transport of large molecules ranging in size from (7.5 to 23 Å). Therefore, paracellular transport of IFN-γ and TNF-α is possible due to their respective hydrodynamic radius of 18.5Å

(Kendrick et al. 1998) and 22Å (Narhi & Arakawa 1987) respectively. The apparent permeability coefficient was calculated for the flux of IFN-γ and TNF-α as $3.12*10^{-6}$ ± 0.47 cm/s and $2.81*10^{-7}$ ± 1.07 cm/s respectively. The larger hydrodynamic radius and secondary structure could account for the lower permeability coefficient of TNF-α at 3 nM or in combination with IFN-γ (Fig 3.1C). The secondary structure of TNF-α consists mainly of β-strands, whereas IFN-γ consists of α-helices which have been shown to contribute to an increase in P_{app} (Chittchang et al. 2002). The permeability coefficient of IFN-γ across Caco-2 monolayers with intact tight junctions was $5.0*10^{-8}$ cm/s and human colonic tissue was $1.9*10^{-5}$ cm/s (Rubas et al. 1996). The P_{app} of IFN-γ decreased by 2 orders of magnitude when there was a disruption in the tight junctions of the monolayer permitting cytokine detection in the apical chamber. The greater permeability of human colonic tissue relative to Caco-2 monolayers for IFN-γ may permit increased flux of IFN-γ across the epithelial barrier at sites of inflammation.

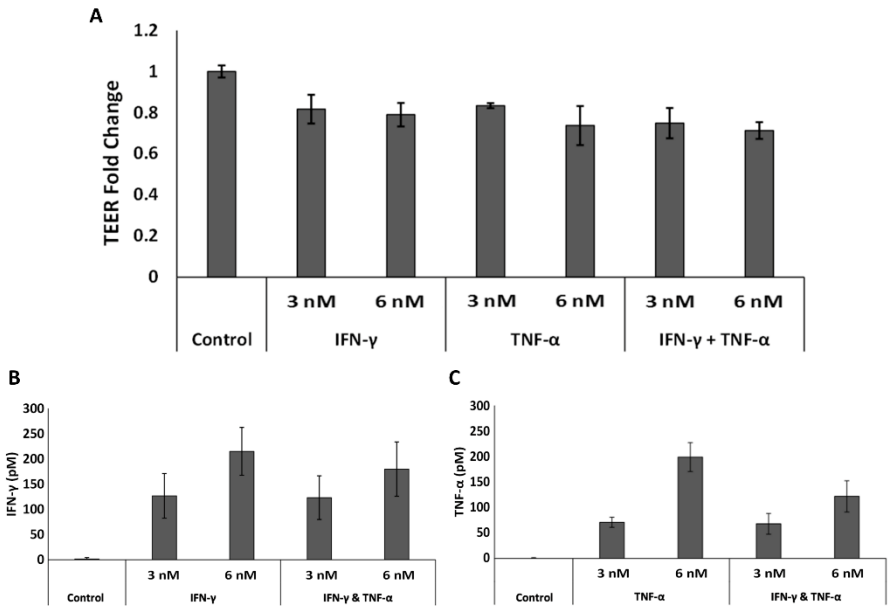

Figure 3.1: IFN-γ and TNF-α reduce barrier function of Caco-2 cell monolayers, permitting transport of cytokines from the basolateral chamber to the apical chamber. (A) Caco-2 monolayers were incubated with no cytokines (control), 3 nM, 6 nM of IFN-γ, TNF-α or in combination, applied to the basolateral chamber. TEER was measured to determine cytokine impact on barrier integrity of tight junctions and apical chamber supernatant was collected at 48 hours. (B) ELISA quantification of apical concentrations (pM) of IFN-γ. (C) ELISA quantification of apical TNF-α (pM). Error bars represent confidence intervals of 95%, (n=9).

Bacterial Detection of IFN-γ and TNF-α

Bacterial strain JW0940-R harboring (pTCA4) or (pTCA6) was used for the detection of IFN-γ and TNF-α. In our previous work, we administered cytokines directly to the bacterial culture; pTCA4 detected IFN-γ at a minimal concentration of 300 pM and pTCA6 detected IFN-γ at 300 pM and TNF-α at 150 pM (Aurand & March 2015). Therefore, we wanted to determine if direct application of the bacterial bioreporter to the Caco-2 monolayer altered the response. Apical supernatant was diluted at a ratio of 1:4 with pTCA4 or pTCA6, (Fig 3.2, A&B) respectively. pTCA4 (Fig 3.2A) did not detect IFN-γ or TNF-α and pTCA6 (Fig 3.2B) detected IFN-γ in the supernatant with the basolateral application of 6 nM. However, when pTCA4 or pTCA6 (Fig 3.2, C&D), respectively, were applied directly to the apical chamber, pTCA4 (Fig 3.2C) was capable of detecting IFN-γ at the higher administered concentrations and pTCA6 detected both IFN-γ and TNF-α (Fig 3.2D).

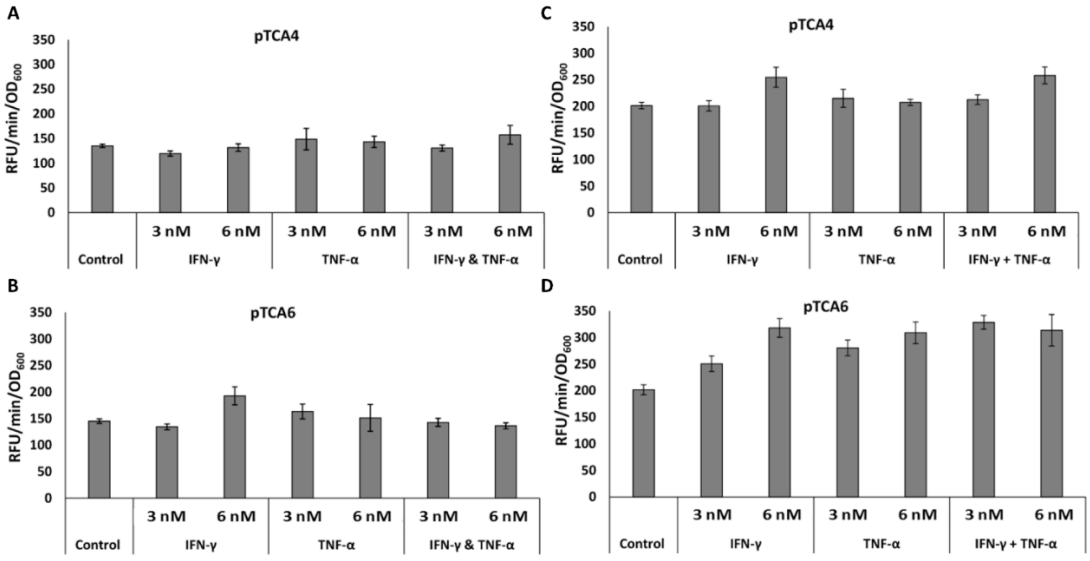

Figure 3.2: Detection of IFN-γ and TNF-α by JW0940-R harboring pTCA4 or pTCA6. β-galactosidase activity of pTCA4 (A) or pTCA6 (B) in response to indirect application of apical supernatant (supernatant removed and diluted 1:4 with bacterial culture), or to direct application of pTCA4 (C) and pTCA6 (D) to the apical chamber. Error bars, represent a CI of 95%, n = 9 per treatment.

Detection of cytokines by the indirect method mimics how the whole cell bioreporter would be used to determine the presence of IFN-γ or TNF-α in a stool sample from an IBD patient. The apical supernatant was added to a bacterial culture under agitation allowing for a more uniform distribution of the cytokine in solution. The whole cell bioreporter was incapable of detecting the inflammatory cytokines within the apical supernatant when added to the bacterial culture at the same concentrations seen by the direct application method. Nevertheless, direct application of the bacterial bioreporter, which is similar to how it would be deployed in the gut, improved the detection of cytokines potentially a result of proximity to the barrier. The bioreporter may settle on the surface of the apical membrane of the Caco-2 monolayer due to a lack of agitation. This settling would result in the exposure of the bacterial bioreporter to higher cytokine concentrations at the interface of the dysfunctional barrier relative to decreasing cytokine concentrations as the distance from the barrier increased. Further, in patients with IBD there is evidence that suggests the mucus barrier diminishes at the sites of inflammation, allowing for bacteria to directly interact with the epithelial barrier (Kleessen et al. 2002; Swidsinski et al. 2007). This breakdown in the mucus barrier at sites of inflammation would permit the engineered bacteria to interact with higher concentrations of inflammatory cytokines at the interface of the leaky epithelial barrier.

Sensitivity of Bacterial Biosensor

IFN-γ and TNF-α concentrations were quantified in the apical chamber by ELISA and the subsequent response of JW0940-R harboring pTCA4 or pTCA6 is

depicted in (Fig 3.3). A fitted line plot of the samples was constructed, and a linear fit model produced acceptable R^2 values. The red dotted lines represent 95% CIs for the mean reporter response. How narrow the confidence intervals are to the trend line depicts the accuracy of the mean response of the engineered strains to IFN-γ or TNF-α. Green dotted lines represent 90% PI of the assay indicating that 90% of individual results will fall within these lines. A PI of 90% was used to determine the concentration threshold where a positive sample will be detected relative to no cytokines with a 5% type one error rate. To do this, the point where the upper PI for no cytokines intersects the lower PI was determined. The cytokine concentration at this intersection represents the concentration threshold for the assay. With a 90% PI, 5% of samples will fall above and 5% below the prediction interval. Therefore in a mixed population of samples, containing samples with no cytokines and samples at the assay threshold (crosshairs on Fig. 3.3), there will be a 5% type one error rate for individual assays (one tailed comparison).

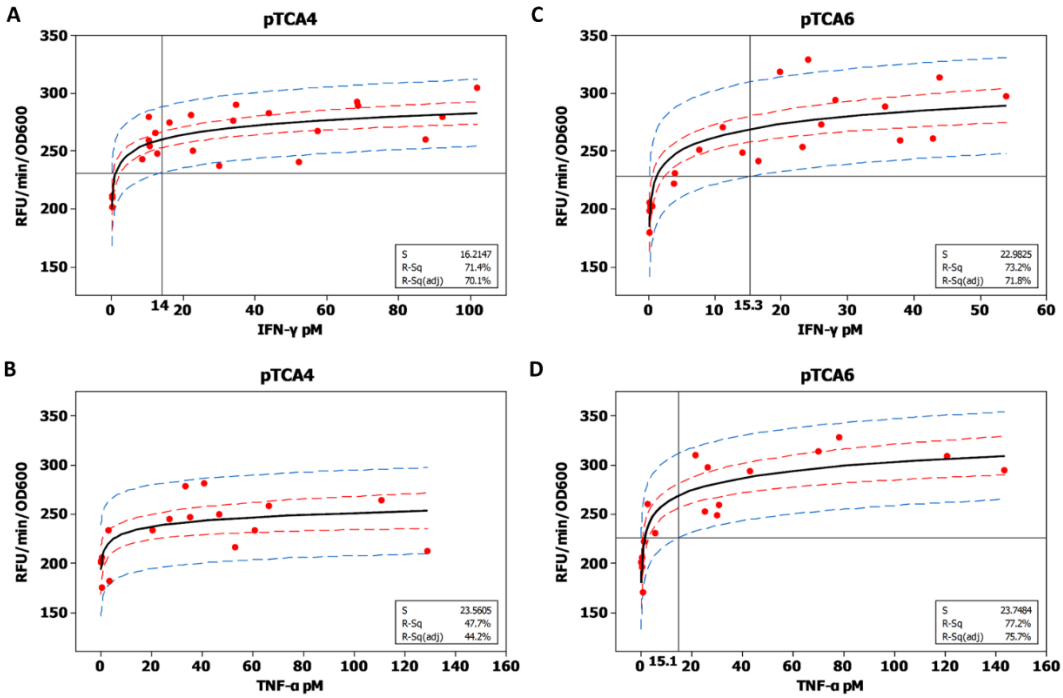

Figure 3.3: Response of JW094-R harboring pTCA4 (A & B) or pTCA6 (C & D**)** to IFN-γ or TNF-α that permeated from the basolateral to apical chamber. A fitted line plot was applied to obtain the trend line. Red dotted lines represent a 95% CI and green dotted lines represent a 90% PI. Crosshairs represent the minimum detectable cytokine threshold concentration with a 5% type one error, $n \geq 15$.

The use of whole cell bioreporters for the detection of disease relevant compounds and pro-inflammatory cytokines in the intestinal tract show great potential as a non-invasive mean to detect disease. The whole cell bacterial sensor harboring pTCA4 was capable of detecting IFN-γ at a threshold concentration of 14 pM. pTCA6 was able to detect IFN-γ and TNF-α at minimum threshold concentrations of 15.3 pM and 15.1 pM respectively with a 5% error (Fig. 3.3). Previously, TNF-α has been detected in the stool of patients diagnosed with IBD at concentrations ranging from 15.8 to 343.8 pM (Braegger et al. 1992), therefore, pTCA6 is well within the observed concentrations for detection of TNF-α. However, IFN-γ concentrations have not been reported in stool samples in IBD patients, which may be a result of the stage of disease progression since it is well established that IFN-γ is involved in IBD (Bisping et al. 2001; Ito et al. 2006; Neurath 2014), and the work presented here indicates that IFN-γ can permeate a "leaky" Caco-2 cell monolayer. Spencer *et al* (2002) conducted a longitudinal study of inflammation progression of colitis in mice and showed that IFN-γ production increases during early stages of inflammation and dissipated at late stages, whereas TNF-α production was constant throughout the disease. This emphasizes the need for a detection system for IFN-γ that can reach the site of inflammation and detect IFN-γ where it is at the highest concentration. Further, the IFN-γ bioreporter could be applied to other diseases such as shigellosis of which IFN-lbγ was present in the stool of patients at concentrations of 17.9 pM to 113 pM of which concentrations increased with duration of the infection (Raqib et al. 1995).

This bioreporter may provide an inexpensive means to monitor IFN-γ and TNF-α concentrations in the gut, in order to detect early stages of inflammation prior

to the development of symptoms in the host. Monitoring of IFN-γ by means of a noninvasive bacterial bioreporter such as our own could improve the quality of life of IBD patients who are in remission by detecting early stages of relapse, permitting intervention to prevent full relapse. Relapse prevention reduces the risk of development of colorectal cancer or other diseases (Binder 2004).

Conclusion

Whole cell bioreporters show great potential as a means for detection of chronic inflammation of the gut. We have shown here that IFN-γ and TNF-α induced barrier dysfunction, permits the diffusion of pro-inflammatory cytokines across a Caco-2 monolayer. Further, IFN-γ and TNF-α were detected by a whole cell bioreporter at higher sensitivity when directly applied to the apical side of the monolayer. Detection of inflammation markers at the site of inflammation could permit an inexpensive means for detection of chronic inflammation in the gut and monitoring over time.

References

Al-Sadi, R., Boivin, M. & Ma, T., 2009. Mechanism of cytokine modulation of epithelial tight junction barrier. *Frontiers in bioscience : a journal and virtual library*, 14, pp.2765–2778. Available at: http://www.ncbi.nlm.nih.gov/pmc/articles/PMC3724223/.

Artursson, P. & Karlsson, J., 1991. Correlation between oral drug absorption in humans and apparent drug permeability coefficients in human intestinal epithelial (Caco-2) cells. *Biochemical and Biophysical Research Communications*, 175(3), pp.880–885. Available at: http://www.sciencedirect.com/science/article/pii/0006291X9191647U.

Aurand, T.C. & March, J.C., 2015. Development of a synthetic receptor protein for sensing inflammatory mediators interferon-γ and tumor necrosis factor-α. *Biotechnology and Bioengineering*, p.n/a–n/a. Available at: http://doi.wiley.com/10.1002/bit.25832.

Aurand, T.C., Russell, M.S. & March, J.C., 2012. Synthetic signaling networks for therapeutic applications. *Current opinion in biotechnology*, 23(5), pp.773–779. Available at: http://www.ncbi.nlm.nih.gov/pubmed/22285057 [Accessed December 23, 2012].

Baba, T. et al., 2006. Construction of Escherichia coli K-12 in-frame, single-gene knockout mutants: the Keio collection. *Molecular systems biology*, 2(1), p.2006.0008. Available at: http://msb.embopress.org/content/2/1/2006.0008.abstract.

Binder, V., 2004. Epidemiology of IBD during the twentieth century: an integrated view. *Best Practice & Research Clinical Gastroenterology*, 18(3), pp.463–479. Available at: http://www.sciencedirect.com/science/article/pii/S1521691803001653.

Bisping, G. et al., 2001. Patients with inflammatory bowel disease (IBD) reveal increased induction capacity of intracellular interferon-gamma (IFN-γ) in peripheral CD8+ lymphocytes co-cultured with intestinal epithelial cells. *Clinical & Experimental Immunology*, 123(1), pp.15–22. Available at: http://dx.doi.org/10.1046/j.1365-2249.2001.01443.x.

Braegger, C.P. et al., 1992. Tumour necrosis factor alpha in stool as a marker of intestinal inflammation. *The Lancet*, 339(8785), pp.89–91. Available at: http://www.sciencedirect.com/science/article/pii/014067369290999J.

Carty, E. et al., 2000. Measurement of in vivo rectal mucosal cytokine and eicosanoid production in ulcerative colitis using filter paper. *Gut* , 46 (4), pp.487–492. Available at: http://gut.bmj.com/content/46/4/487.abstract.

Chittchang, M. et al., 2002. Poly(L-lysine) as a model drug macromolecule with which to investigate secondary structure and microporous membrane transport, part 2: diffusion studies. *Journal of Pharmacy and Pharmacology*, 54(11), pp.1497–1505. Available at: http://dx.doi.org/10.1211/002235702108.

Cox, D.S. et al., 2001. Enhancing the permeation of marker compounds and enaminone anticonvulsants across Caco-2 monolayers by modulating tight junctions using zonula occludens toxin. *European Journal of Pharmaceutics and*

Biopharmaceutics, 52(2), pp.145–150. Available at: http://www.sciencedirect.com/science/article/pii/S0939641101001722.

Fish, S.M., Proujansky, R. & Reenstra, W.W., 1999. Synergistic effects of interferon γ and tumour necrosis factor α on T84 cell function. *Gut* , 45 (2), pp.191–198. Available at: http://gut.bmj.com/content/45/2/191.abstract.

Groschwitz, K.R. & Hogan, S.P., 2009. Intestinal barrier function: Molecular regulation and disease pathogenesis. *Journal of Allergy and Clinical Immunology*, 124(1), pp.3–20. Available at: http://www.sciencedirect.com/science/article/pii/S0091674909008641.

Hanauer, S.B., 2006. Inflammatory bowel disease: Epidemiology, pathogenesis, and therapeutic opportunities. *Inflammatory Bowel Diseases*, 12(5), pp.S3–S9. Available at: http://dx.doi.org/10.1097/01.MIB.0000195385.19268.68.

Ito, R. et al., 2006. Interferon-gamma is causatively involved in experimental inflammatory bowel disease in mice. *Clinical & Experimental Immunology*, 146(2), pp.330–338. Available at: http://dx.doi.org/10.1111/j.1365-2249.2006.03214.x.

Kendrick, B.S. et al., 1998. A transient expansion of the native state precedes aggregation of recombinant human interferon-γ. *Proceedings of the National Academy of Sciences* , 95 (24), pp.14142–14146. Available at: http://www.pnas.org/content/95/24/14142.abstract.

Kleessen, B. et al., 2002. Mucosal and Invading Bacteria in Patients with Inflammatory Bowel Disease Compared with Controls. *Scandinavian Journal of*

Gastroenterology, 37(9), pp.1034–1041. Available at: 10.1080/003655202320378220.

Ma, T.Y. et al., 2004. TNF-α-induced increase in intestinal epithelial tight junction permeability requires NF-κB activation. *American Journal of Physiology - Gastrointestinal and Liver Physiology*, 286(3), pp.G367–G376. Available at: http://ajpgi.physiology.org/content/286/3/G367.abstract.

MacDonald, T.T. et al., 1990. Tumour necrosis factor-alpha and interferon-gamma production measured at the single cell level in normal and inflamed human intestine. *Clinical and Experimental Immunology*, 81(2), pp.301–305. Available at: http://www.ncbi.nlm.nih.gov/pmc/articles/PMC1535044/.

Madara, J.L. & Stafford, J., 1989. Interferon-gamma directly affects barrier function of cultured intestinal epithelial monolayers. *Journal of Clinical Investigation*, 83(2), pp.724–727. Available at: http://www.ncbi.nlm.nih.gov/pmc/articles/PMC303735/.

Molodecky, N.A. et al., 2012. Increasing Incidence and Prevalence of the Inflammatory Bowel Diseases With Time, Based on Systematic Review. *Gastroenterology*, 142(1), pp.46–54.e42. Available at: http://www.sciencedirect.com/science/article/pii/S0016508511013783.

Narhi, L.O. & Arakawa, T., 1987. Dissociation of recombinant tumor necrosis factor-α studied by gel permeation chromatography. *Biochemical and Biophysical Research Communications*, 147(2), pp.740–746. Available at: http://www.sciencedirect.com/science/article/pii/0006291X87909922.

Neurath, M.F., 2014. Cytokines in inflammatory bowel disease. *Nat Rev Immunol*, 14(5), pp.329–342. Available at: http://dx.doi.org/10.1038/nri3661.

Ramsay, J.P. et al., 2011. A quorum-sensing molecule acts as a morphogen controlling gas vesicle organelle biogenesis and adaptive flotation in an enterobacterium. *Proceedings of the National Academy of Sciences* , 108 (36), pp.14932–14937. Available at: http://www.pnas.org/content/108/36/14932.abstract.

Raqib, R. et al., 1995. Cytokine Secretion in Acute Shigellosis Is Correlated to Disease Activity and Directed More to Stool than to Plasma. *Journal of Infectious Diseases* , 171 (2), pp.376–384. Available at: http://jid.oxfordjournals.org/content/171/2/376.abstract.

Rescigno, M., 2011. The intestinal epithelial barrier in the control of homeostasis and immunity. *Trends in Immunology*, 32(6), pp.256–264. Available at: http://www.sciencedirect.com/science/article/pii/S1471490611000585.

Rubas, W. et al., 1996. Flux measurements across Caco-2 monolayers may predict transport in human large intestinal tissue. *Journal of Pharmaceutical Sciences*, 85(2), pp.165–169. Available at: http://dx.doi.org/10.1021/js950267+.

Spencer, D.M. et al., 2002. Distinct inflammatory mechanisms mediate early versus late colitis in mice. *Gastroenterology*, 122(1), pp.94–105. Available at: http://www.sciencedirect.com/science/article/pii/S0016508502653715.

Steidler, L. et al., 2000. Treatment of Murine Colitis by Lactococcus lactis Secreting Interleukin-10. *Science* , 289 (5483), pp.1352–1355. Available at: http://www.sciencemag.org/content/289/5483/1352.abstract.

Swidsinski, A. et al., 2007. Comparative study of the intestinal mucus barrier in normal and inflamed colon. *Gut* , 56 (3), pp.343–350. Available at: http://gut.bmj.com/content/56/3/343.abstract.

Wang, F. et al., 2005. Interferon-γ and Tumor Necrosis Factor-α Synergize to Induce Intestinal Epithelial Barrier Dysfunction by Up-Regulating Myosin Light Chain Kinase Expression. *The American Journal of Pathology*, 166(2), pp.409–419. Available at: http://www.ncbi.nlm.nih.gov/pmc/articles/PMC1237049/.

Watson, C.J. et al., 2005. Interferon-γ selectively increases epithelial permeability to large molecules by activating different populations of paracellular pores. *Journal of Cell Science* , 118 (22), pp.5221–5230. Available at: http://jcs.biologists.org/content/118/22/5221.abstract.

Watson, C.J., Rowland, M. & Warhurst, G., 2001. Functional modeling of tight junctions in intestinal cell monolayers using polyethylene glycol oligomers. *American Journal of Physiology - Cell Physiology*, 281(2), pp.C388–C397. Available at: http://ajpcell.physiology.org/content/281/2/C388.abstract.

CHAPTER FOUR

Detection of Uric Acid by a Novel Synthetic Reporter System Deployed in *E. coli**

* Thomas Christopher Aurand, Christopher Mancuso, John C. March

Abstract

Hyperuricemia is defined as blood serum concentrations of uric acid above 360 μM and has been implicated to have an impact on the health of an individual, potentially resulting in Gout, renal disease, cardiovascular disease and other chronic diseases. Here, a bioreporter system was developed to monitor uric acid concentrations. The transcriptional regulator, *pucR*, of the purine catabolism pathway of *Bacillus subtilis* was used to develop a synthetic promoter in which the *pucR* box regulates GFP expression in the presence of uric acid. This system was capable of differentiating between healthy and hyperuricemic concentrations of uric acid estimated to be present in the intestinal lumen.

Introduction

The prevalence of hyperuricemia is on the rise, affecting 8.3 million adults in the United States and is defined as serum uric acid concentration exceeding 360 μM for women and 386 μM for men (Klemp et al., 1997; Zhu et al., 2011). Elevated concentrations of uric acid in the blood have been linked to Gout, renal disease, cardiovascular disease, metabolic disease and hypertension (Kutzing and Firestein, 2008). The development of hyperuricemia is associated with a number of factors, such as purine rich diets, excessive alcohol consumption and genetic predisposition (Nuki and Simkin, 2006). Gout most frequently occurs in patients between the ages of 30 to 50, directly impacting their quality of life and reducing the productivity of the population while increasing costs to the general public (Wertheimer et al., 2013).

Uric acid is the end product of the purine degradation pathway in humans and serum concentrations can be altered by dietary and lifestyle changes. Serum of

healthy individuals contain uric acid concentrations of 120 μM – 360 μM (Kutzing and Firestein, 2008). However, concentrations at the high end of this range and above may lead to the accumulation of monosodium urate crystals in the joints, resulting in a form of arthritis known as Gout. Even minor elevated levels can induce vasoconstriction and hypertension (Sanchez-Lozada et al., 2005). An imbalance in the production and excretion of uric acid leads to the development of hyperuricemia. The primary route of excretion occurs by the renal pathway, accounting for 70% of the daily turnover. The remaining portion is removed directly through the intestine in which the highest secretion rate was observed in the ileum (Hosomi et al., 2012). However, concentrations of uric acid observed in stool are low due to bacterial based uricolysis, accounting for a 75% loss of uric acid during transit (Lin et al., 2002; Yu et al., 2004). An estimate of the intestinal steady state uric acid concentration is required to develop a bioreporter to monitor elevated uric acid concentrations.

The development of bacterial based synthetic circuits for the detection and treatment of diseases become a topic of interest. Engineered bacterial systems utilize genetic components to detect environmental cues and respond in a measurable manner. A previously developed system in our laboratory, for detection of the inflammatory cytokines interferon-γ (IFN-γ) and tumor necrosis factor-α (TNF-α). A chimeric protein expressed on the surface of *Escherichia coli* was engineered to bind IFN-γ and TNF-α, which subsequently induced *lacZ* expression under control of the *pspA* promoter (Aurand and March, 2015). In addition, Kemmer *et al* (2010) developed a synthetic mammalian circuit to monitor serum uric acid concentrations and control uricase production to reduce elevated uric acid levels in the blood to

homeostatic levels. However, a potential downside to this system is it requires a prosthetic device containing the engineered cells to be implanted into the patient to monitor blood uric acid levels. Current treatments for hyperuricemia focus on limiting the inflammation produced during flare ups by the use of nonsteroidal anti-inflammatory drugs or colchicine, however, these treatments do not reduce serum uric acid concentrations (Gliozzi et al., 2015)

A noninvasive whole cell bioreporter system that could be deployed in the gastrointestinal tract to monitor uric acid concentrations was developed here. The whole cell bioreporter was constructed using components of the purine catabolism pathway (*pucR* and *pucJKLM*) of *Bacillus subtilis*, a gram-positive bacterium that utilizes purines as a source of nitrogen. The purine catabolism pathways is controlled by the transcriptional regulator, PucR. When the transcriptional regulator PucR is bound to uric acid or one of its degradation products, allantoin or allantoic acid it exhibits binding location-dependent transcriptional regulation (Beier et al., 2002). PucR activates the transcription of the *pucJKLM operon*, controlling uric acid uptake and degradation, however, PucR bound to uric acid represses the expression of *pucA* and *pucR* (Schultz et al., 2001). Transcriptional regulation is achieved by a *pucR* binding site, referred to as the *pucR* box (5'- WWCNTTGGTTAA-3'). The *pucR* box is found upstream of the -35 sequence when in an activating orientation and overlapping the -35 promoter element (*pucA*) or downstream of the transcriptional start site in a repressing orientation (Beier et al., 2002), where it blocks the movement of RNA polymerase.

The proposed whole cell bioreporter system for the detection of uric acid

consists of *pucR* constitutively expressed and a reporter construct utilizing a synthetic promoter in which the *pucR* box controls the expression of green fluorescence protein (GFP). This proposed system could support the future development of a diagnostic system or for monitoring uric acid in the intestinal lumen and responding with the production of a therapeutic compound.

Materials and Methods

Bacterial Strains and chemicals

Host strain, *E. coli* Dh5α was used for all subsequent recombinant DNA manipulation and expression. *B. subtilis* 168, (ATCC® 23857), a gift from the Wiedmann group, (Cornell University) was used for amplification of the *pucR* gene and the *pucJKLM* operon using the Q5 High Fidelity Polymerase New England Biolabs (Ipswich, MA). Bacterial strains, plasmids, and primers used in this study are listed in (Table 4.1). Cultures were grown at 37°C in Luria-Bertani broth (LB), supplemented with ampicillin at a final concentration of 100 μg/mL, Fisher Scientific (Fair Lawn, NJ) and chloramphenicol at final concentration of 34 μg/mL, VWR International (Radnor, PA). A 100 mM stock solution of uric acid, Amresco (Solon, OH) was used in all experiments and diluted as required.

Plasmid construction

The *pucR* expression vector, (pPUCR) was constructed by linearizing pACYC184 using primers pucR-184 lin F and pucR-184 lin R to remove Tc^R and the Tc^R promoter while maintaining the 3' termination region using Q5 High Fidelity Polymerase, New England Biolabs (Ipswich, MA). *pucR* and its promoter region were amplified with Q5 High Fidelity Polymerase, New England Biolabs (Ipswich, MA),

such that the amplicon contained 15bp homologous regions to the linearized pACYC184 with primers, pucR ins F and pucR ins R. Linearized vector and insert were assembled using the Gibson Assembly Master Mix Kit, New England Biolabs (Ipswich, MA) and transformed into chemically competent *E. coli* Dh5α.

The reporter construct implemented a rationally designed 149bp synthetic promoter (pucproGFP), Integrated DNA Technologies (Coralville, IA). The constitutive *camR* promoter was used as a backbone in which the *pucR* box, TATCATTGGTTAA was inserted in frame, replacing the spacer region between the -35 and -10 consensus sequences. pGFPuv was linearized by primers, pGFPuv lin F and pGFPuv lin R using Q5 High Fidelity Polymerase, New England Biolabs (Ipswich, MA), removing the GFPuv promoter. The GFPuv promoter was replaced with the synthetic promoter, pucproGFP, assembled using the Gibson Assembly Master Mix Kit, New England Biolabs (Ipswich, MA) yielding, pPRGFP and transformed into chemically competent *E. coli* Dh5α. All Constructs were screened by PCR, selected colonies were sequenced by the Cornell Biotechnology Resource Center (Ithaca, NY). Verified constructs of pPUCR and pPRGFP were co-transformed into chemically competent *E. coli* Dh5α for subsequent experiments.

Table 4.1: Strains, plasmids and PCR primers used in this study

Strain	Genotype or Decription	Source
E. coli Dh5α	*fhuA2 Δ(argF-lacZ)U169 phoA glnV44 Φ80 Δ(lacZ)M15 gyrA96 recA1 relA1 endA1 thi-1 hsdR17*	March Group
B. sutilis 168	*trpC2*	Wiedmann Group
Plasmid		
pACYC184	*camR, tetR*	March Group
pGFPuv	*GFPuv, ampR*	March Group
pPUCR	pACYC184 backbone, *tetR* replaced with *pucR* of *B. subtilis*	This work
pPRGFP	pGFPuv backbone, in which the GFPuv promoter is replaced with a synthetic promoter consisting of pucR consensus box placed between -10 and -35 RBS of the camR promoter	This work
Primers		
pucproGFP	GTTGGCCGATTCATTAATGCGGCACGTAAGATATCATTGGTTAAACCATAATGAAATAAGATCACT ACCGGGCGTATTTTTTGAGTTATCGAGATTTTCAGGAGCTAAGGAAGCTAAAATGAGTAAAGGAGAAG AACTTTTCACTGGAG	
pGFPuv lin F	GGTGCCTCACTGATTAAGCATTGGTAACTGTCAGACCAAGTTTACTC	
pGFPuv lin R	GAGTAAACTTGGTCTGACAGTTACCAATGCTTAATCAGTGAGGCACC	
pucR ins F	GTAGCACCTGAAGTCAGCCCCATGTCAGTTTATGTAACACAACCAG	
pucR ins R	GAGGCAGACAAGGTATAGGGCGGTGTCATTGGATACAGTAGCTG	
pucR-184 lin F	GCCCTATACCTTGTCTGCCTC	
pucR-184 lin R	GGCTGACTTCAGGTGCTACATTTG	

GFP testing

Time course and end point fluorescence assays were used to characterize the response of the reporter construct. Cultures were grown overnight at 37°C in LB supplemented with appropriate antibiotics for vector maintenance. Overnight cultures were diluted 1:25 with M9 media supplemented with thiamine. For time course assays, uric acid was added to cultures at a final concentration of 250 μM and aliquoted into clear bottom 96 well black polymer microplate, Thermo Scientific Nunc (Rochester, NY). Microplates were shaken at 37°C; cell density (600nm) and fluorescence, (excitation and emission of 395nm and 509nm respectively) were monitored by a Biotek Synergy 4 plate reader, BioTek (Winooski, VT) every 20 minutes for 12 hours, to optimize the end point assay. End point assays were used to measure response of all constructs at 0 μM, 50 μM and 75 μM of uric acid. Dose response of the bioreporter strain, *E. coli* DH5α harboring pPUCR and pPRGFP was determined over a range of 0 μM – 250 μM of uric acid. Cultures were incubated for 6 hours as previously optimized and fluorescence was measured. All fluorescence measurements were reported as relative fluorescence units (RFU) normalized by OD_{600}.

Statistics

Error bars represent 95% confidence intervals (CI) of 8 biological replicates, (n=8). Student's t-tests were conducted using Minitab®17 (State College, PA) between uninduced and induced strains, p-values < 0.05, 0.01 are represented as * and ** respectively. Using Minitab®17 (State College, PA) results were analyzed by a one-way analysis of variance (ANOVA) test combined with a post-hoc Tukey HSD

for multiple comparison with a confidence level of 95%.

Results and Discussion

The daily uric acid turnover rate for a healthy individual is approximately 780 mg/day, of which 546 mg/day (70%) is excreted by the renal system, 234 mg/day (30%) is removed by the intestine (Sorensen, 1965). Furthermore, for cases of hyperuricemia in which increased uric acid production is observed, the renal excretion pathway will remove uric acid at a rate of >1 g/day and the intestinal pathway removes 429 mg/day (Yu et al., 2004). In order to estimate the steady state intestinal concentration of uric acid, a mass balance can be performed

$$\frac{dm_{\mathrm{u}}}{dt} = \frac{d(V_{\mathrm{int}}[U])}{dt} = 0 = s - q[U] - k$$

where m_u is the mass of uric acid in the intestine, V_{int} is the intestinal volume, [U] is the concentration of uric acid, s is the intestinal secretion rate of uric acid (0.1625 mg/min for healthy and 0.2979 mg/min for hyperuricemia), q is the intestinal flow rate which varies between 5 and 20 mL/min depending on time since last meal (Fine et al., 1995), and k is the degradation rate constant. Setting the degradation rate equal to three times the elimination by flow because 75% of the total uric acid excreted into the intestine is degrade during transit by bacterial uricolysis yields

$$\frac{d(V_{\mathrm{int}}[U])}{dt} = 0 = s - 4q[U]$$

and the steady state concentration at the long term flow rate of 5 mL/min is found to be $8.125*10^{-3}$ mg/mL (48.3 μM) for healthy individuals and $1.49*10^{-2}$ mg/mL (≥ 88.7 μM) for hyperuricemia patients. However, these values may be an underestimate due to compensation by the intestine for decreased renal elimination

(Dincer, H. Erhan, Ayse P. Dincer, 2002; Vaziri et al., 1995). This deduction makes gross assumptions of equal flow rate in the small and large intestine, nevertheless, it establishes a detection threshold for intestinal uric acid.

A whole cell bioreporter with the capacity to differentiate between healthy and hyperuricemic uric acid concentrations was developed using the *pucR* transcriptional regulator and a rationally designed synthetic promoter regulated by a PucR uric acid complex. In order to achieve this, *pucR* was constitutively expressed in the bioreporter system. Furthermore, *pucR* expression is under negative autoregulation, as observed by Schultz *et al* (2001) in which the addition of allantoin reduced *pucR* expression four fold. Autoregulation of *pucR* is controlled by two *pucR* boxes; one located downstream of the transcriptional start site, which partially represses *pucR* expression and a second *pucR* box overlapping the -35 sequence, both require binding of the uric acid/PucR complex to the *pucR* boxes to repress expression (Beier et al., 2002; Schultz et al., 2001).

An initial reporter was constructed, using the *pucJ* promoter which contained a *pucR* box upstream of the -35 core promoter site, in an activator orientation, however, expression was downregulated in this system (data not shown) which could be the result of *pucR* negative autoregulation. This led to the development of the pucproGFP synthetic promoter, in which the *pucR* box, "TATCATTGGTTAA" was placed between the -10 and -35 sequences of a constitutively expressed chloramphenicol promoter, (Fig 4.1). In the presence of uric acid, PucR represses its own expression by binding to the *pucR* box overlapping the -35 sequence. We hypothesized that the promoter designed here would constitutively express GFP in the absence of uric acid

and expression would be downregulated the PucR/uric acid complex binding to the *pucR* box located in the spacer region of the synthetic promoter, preventing transcription.

Figure 4.1: The synthetic promoter, pucproGFP consists of the *camR* promoter as the promoter backbone in which the spacer region between the -10 and -35 consensus sequence is replaced by the *pucR* box.

To test the response of the bioreporter, cultures were induced with uric acid at concentrations of 0 μM, 50 μM and 75 μM (Fig 4.2). Controls containing either the *pucR* expression vector or the reporter construct, pPRGFP had no significant response to uric acid relative to the native strain background (Fig 4.2). The bioreporter, harboring both pPRGFP and the *pucR* expression vector, showed an increase in basal expression relative to control strains in the absence of uric acid. Furthermore, contrary to our hypothesis, the addition of uric acid induced expression of the synthetic promoter driving GFP production. This result could relate to the negative autoregulation of *pucR* or the more probable explanation is due to strand orientation of the *pucR* box. Induction of GFP expression when the PucR-uric acid complex binds to the *pucR* box may result in a beneficial conformational changes of the -10 and -35 region enhancing RNA polymerase assembly (Brown et al., 2003; Gilbert, 1976).

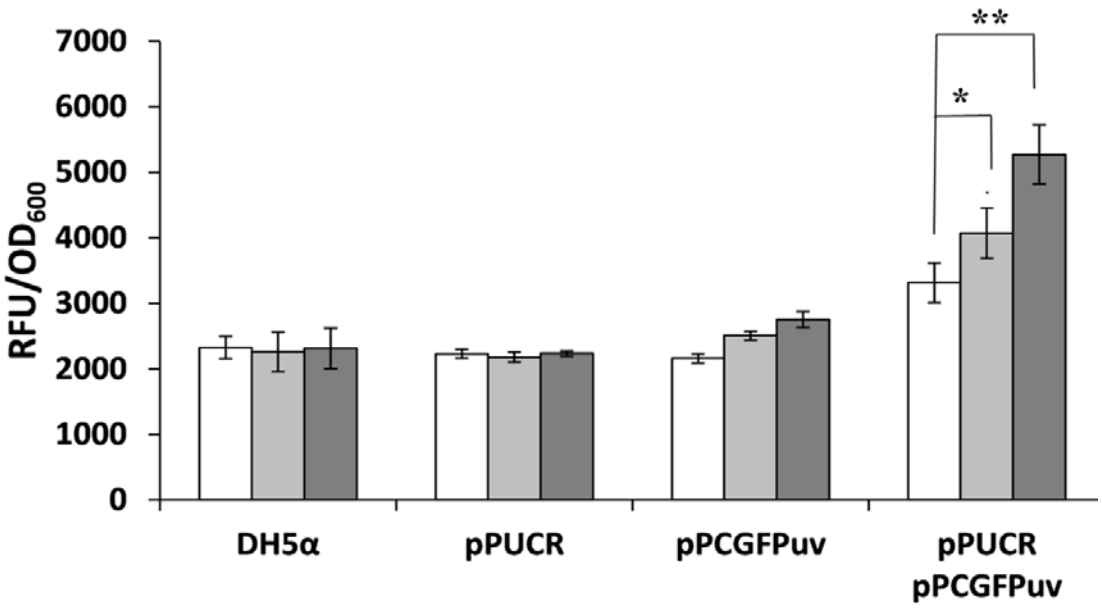

Figure 4.2: Response of constructs to 0 μM (white), 50 μM (light gray) and 75 μM (dark gray) of uric acid measured by GFPuv production (RFU) and normalized by cell density (OD_{600}) after 6 hours of induction. Error bars represent 95% confidence intervals, * indicates a p-value <0.05 and ** has a p-value <0.01 determined by a student T-test comparing induced to uniduced RFU/OD_{600}, n = 12.

The dose response of the whole cell bioreporter to uric acid over a concentration range of 0 μM – 250 μM is depicted in (Fig 4.3). The response of the bioreporter was analyzed using a one-way analysis of variance (ANOVA) test combined with a post-hoc Tukey HSD for multiple comparison at a 95% confidence level relative to 50 μM of uric acid. The uric acid concentration of 48.3 μM was proposed as the median concentration present in the intestine of a healthy individual. Therefore, a concentration of 50 μM (the first concentration tested above 48.3 μM) was selected as the baseline for healthy individuals. A concentration of 88.7 μM uric acid was the calculated threshold concentration to be considered hyperuricemic. The whole cell bioreporter could significantly differentiate between healthy uric acid concentration (50 μM) and concentrations of 75 μM and above of uric acid. Further, significance improved as concentrations of uric acid increased.

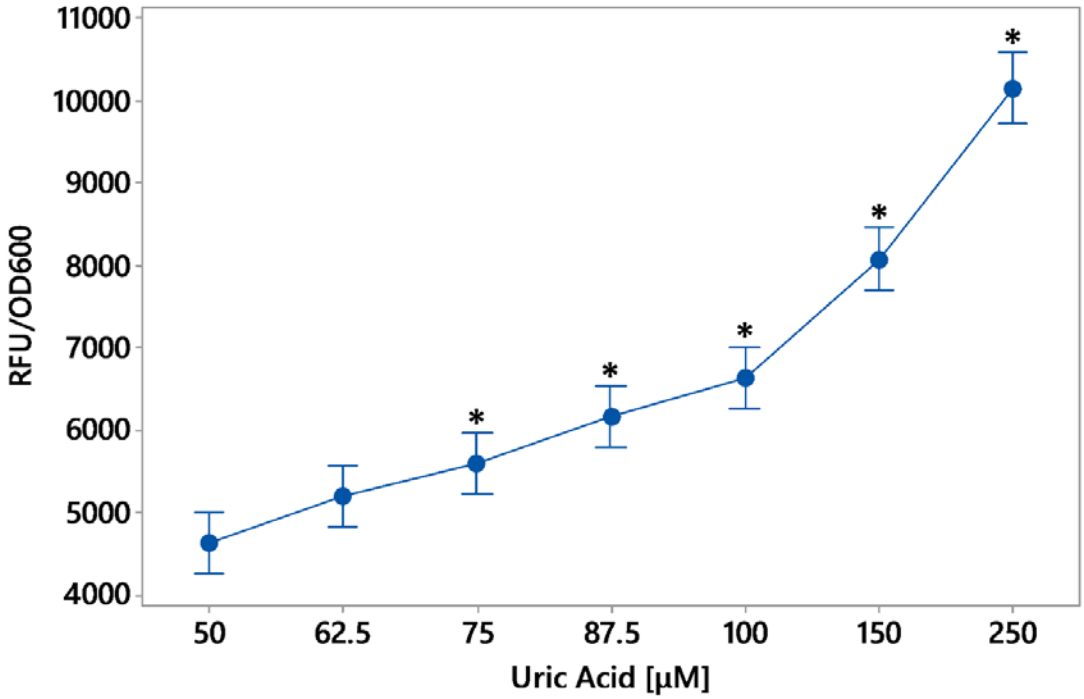

Figure 4.3: Dose response of the engineered bioreporter to uric acid (0 µM – 250 µM) measured as RFU and normalized by culture density, OD_{600}. One way ANOVA plot combined with a post-hoc Tukey HSD test, * indicate significance level of 95% relative to 50 µM uric acid, n = 8.

The bioreporter developed here showed a significant increase in GFP production at the threshold concentration calculated for hyperuricemia relative to the calculated healthy intestinal concentration. A previous bioreporter developed in our lab for the detection of IFN-γ showed in an *in vitro* model of epithelial barrier dysfunction, direct application of the bioreporter to the apical chamber or "lumen" of the *in vitro* model, the detection threshold of the bioreporter was significantly improved (Aurand et al., 2015). Direct application of the bioreporter developed here to an *in vitro* model of intestinal excretion of uric acid may improve the magnitude of response seen between healthy and hyperuricemic concentrations.

This is the first time the purine catabolism system of *B. subtilis* has been used to develop a bioreporter to monitor environmental concentrations of uric acid. This provides a tool for the future development of a system to monitor elevated concentrations uric acid prior to uricolysis in the intestinal lumen. Further, the bioreporter developed here could be integrated with other systems to detect or monitor the progression of increasingly complex conditions such as cardiovascular disease or metabolic syndrome. Lastly, the bioreporter could be engineered to produce recombinant compounds, to reduce production and renal reabsorption of uric acid, for the long term treatment of hyperuricemia (Gliozzi et al., 2015).

References

Aurand TC, March JC. 2015. Development of a synthetic receptor protein for sensing inflammatory mediators interferon-γ and tumor necrosis factor-α. *Biotechnol. Bioeng.*:n/a–n/a. http://doi.wiley.com/10.1002/bit.25832.

Aurand TC, Russell MS, Costello CM, March JC. 2015. In vitro Detection of Interferon-γ and Tumor Necrosis Factor-α by a Whole Cell Synthetic Detection System.

Beier L, Nygaard P, Jarmer H, Saxild HH. 2002. Transcription Analysis of the Bacillus subtilis PucR Regulon and Identification of a cis-Acting Sequence Required for PucR-Regulated Expression of Genes Involved in Purine Catabolism. *J. Bacteriol.* **184** :3232–3241. http://jb.asm.org/content/184/12/3232.abstract.

Brown NL, Stoyanov J V, Kidd SP, Hobman JL. 2003. The MerR family of transcriptional regulators. *FEMS Microbiol. Rev.* **27**:145–163. http://dx.doi.org/10.1016/S0168-6445(03)00051-2.

Dincer, H. Erhan, Ayse P. Dincer and DJL. 2002. Asymptomatic hyperuricemia: To treat or not to treat. *Cleve. Clin. J. Med.* **69**:594–608.

Fine KD, Santa Ana CA, Porter JL, Fordtran JS. 1995. Effect of changing intestinal flow rate on a measurement of intestinal permeability. *Gastroenterology* **108**:983–989. http://www.sciencedirect.com/science/article/pii/0016508595901930.

Gilbert W. 1976. Starting and stopping sequences for the RNA polymerase. *Cold Spring Harb. Monogr. Arch.* **6**:193–205.

Gliozzi M, Malara N, Muscoli S, Mollace V. 2015. The treatment of hyperuricemia. *Int. J. Cardiol.* http://www.sciencedirect.com/science/article/pii/S016752731530317X.

Hosomi A, Nakanishi T, Fujita T, Tamai I. 2012. Extra-Renal Elimination of Uric Acid via Intestinal Efflux Transporter BCRP/ABCG2. *PLoS One* **7**:e30456. http://dx.doi.org/10.1371%2Fjournal.pone.0030456.

Kemmer C, Gitzinger M, Daoud-El Baba M, Djonov V, Stelling J, Fussenegger M. 2010. Self-sufficient control of urate homeostasis in mice by a synthetic circuit. *Nat Biotech* **28**:355–360. http://dx.doi.org/10.1038/nbt.1617.

Klemp P, Stansfield S, Castle B, Robertson M. 1997. Gout is on the increase in New Zealand. *Ann. Rheum. Dis.* **56**:22–26. http://www.ncbi.nlm.nih.gov/pmc/articles/PMC1752259/.

Kutzing MK, Firestein BL. 2008. Altered Uric Acid Levels and Disease States. *J. Pharmacol. Exp. Ther.* **324** :1–7. http://jpet.aspetjournals.org/content/324/1/1.abstract.

Lin J-L, Tan D-T, Ho H-H, Yu C-C. 2002. Environmental lead exposure and urate excretion in the general population. *Am. J. Med.* **113**:563–568. http://www.sciencedirect.com/science/article/pii/S0002934302012962.

Nuki G, Simkin PA. 2006. A concise history of gout and hyperuricemia and their treatment. *Arthritis Res. Ther.* **8 Suppl 1**:S1. http://arthritis-research.com/content/8/S1/S1.

Sanchez-Lozada LG, Tapia E, Santamaria J, Avila-Casado C, Soto V, Nepomuceno T, Rodriguez-Iturbe B, Johnson RJ, Herrera-Acosta J. 2005. Mild hyperuricemia

induces vasoconstriction and maintains glomerular hypertension in normal and remnant kidney rats. *Kidney Int* **67**:237–247. http://dx.doi.org/10.1111/j.1523-1755.2005.00074.x.

Schultz AC, Nygaard P, Saxild HH. 2001. Functional Analysis of 14 Genes That Constitute the Purine Catabolic Pathway in Bacillus subtilis and Evidence for a Novel Regulon Controlled by the PucR Transcription Activator. *J. Bacteriol.* **183** :3293–3302. http://jb.asm.org/content/183/11/3293.abstract.

Sorensen LB. 1965. Role of the intestinal tract in the elimination of uric acid. *Arthritis Rheum.* **8**:694–706. http://dx.doi.org/10.1002/art.1780080429.

Vaziri ND, Freel RW, Hatch M. 1995. Effect of chronic experimental renal insufficiency on urate metabolism. *J. Am. Soc. Nephrol.* **6** :1313–1317. http://jasn.asnjournals.org/content/6/4/1313.abstract.

Wertheimer A, Morlock R, Becker MA. 2013. A Revised Estimate of the Burden of Illness of Gout(). *Curr. Ther. Res. Clin. Exp.* **75**:1–4. http://www.ncbi.nlm.nih.gov/pmc/articles/PMC3898191/.

Yu K-H, Luo S-F, Tsai W-P, Huang Y-Y. 2004. Intermittent elevation of serum urate and 24-hour urinary uric acid excretion. *Rheumatol.* **43** :1541–1545. http://rheumatology.oxfordjournals.org/content/43/12/1541.abstract.

Zhu Y, Pandya BJ, Choi HK. 2011. Prevalence of gout and hyperuricemia in the US general population: The National Health and Nutrition Examination Survey 2007–2008. *Arthritis Rheum.* **63**:3136–3141. http://dx.doi.org/10.1002/art.30520.

CHAPTER FIVE

Conclusion

The use of synthetic biology to develop novel genetic circuits for the detection of biologically relevant concentrations of disease biomarkers has become a broad topic of interest. With the increasing costs and occurrence of non-communicable diseases, new methods to monitor disease progression are necessary and whole cell bioreporters could provide a solution to this need (Mendis. et al., 2014). However, at this time there are no synthetically developed biological therapeutics that have been approved by the FDA, although there are a few which have completed phase one trails and are currently in phase two trials. For example, Intrexon® has one such treatment for oral mucositis (AG013), a common complication of chemotherapy, of which the mucosal lining of the mouth breaks down. AG013 is an engineered strain of *L. lactis,* designed to constitutively express and secrete human trefoil factor-1, a peptide involved in protecting and healing the mucosa of the mouth. Results of a phase 1b trial of orally administered AG013 showed a 35% reduction in the number of days a patient presented ulcerative oral mucositis relative to placebo controls (Limaye et al., 2013). Currently, the engineered probiotics in clinical trials constitutively express and secrete therapeutic compounds. Hence, there is a need to develop bacteria based extracellular sensors that could be used to control the production of therapeutic compounds in response to environmentally available disease biomarkers.

Therefore, the research presented in this dissertation had two overall goals: (1) develop a whole cell bioreporter for the detection of the inflammatory cytokines IFN-γ, TNF-α and test the detection capacity of the whole cell bioreporter in an

in vitro model of a dysfunctional intestinal barrier; and (2) develop a whole cell biosensor for the detection of uric acid at estimated concentrations present in the intestinal lumen of hyperuricemic individuals. To pursue these goals, inspiration for the development of the sensor/reporter systems was gleaned from other bacterial gene networks. Synthetic biology techniques and concepts, were harnessed to design these novel bacterial based sensor systems as building blocks for the future development and deployment of environmentally responsive therapeutics.

In order to achieve the first goal of developing a whole cell bioreporter system for IFN-γ and TNF-α, a chimeric outer membrane protein expressed in *E. coli* had to be engineered to bind the inflammatory cytokines. Therefore, the extracellular peptide fragment(s) of OprF, an outer membrane protein of *P. aeruginosa* capable of binding IFN-γ were selected to replace the extracellular loops of the outer membrane protein, OmpA of *E. coli*. Peptide fragments corresponding to amino acids 198-237 of OprF had the greatest binding capacity for IFN-γ. Further, in combination with the identified peptide fragment, amino acids 257-275 or 241-261 of OprF, elicited a detectable response to TNF-α. The identification of the peptide fragments of OprF which bind IFN-γ and interact with TNF-α, expressed as a chimeric OmpA/OprF construct, produced the inflammatory cytokine sensor necessary for monitoring extracellular concentrations of IFN-γ and TNF-α. The identification of these peptide fragments of OprF, a major contributor to the pathogenicity of *P. aeruginosa,* may permit the development of novel therapeutics or be used as a target to hinder cellular adherence and production of virulence related factors.

The second component necessary to achieve the first goal, required the

development of a reporter construct that transduced binding of IFN-γ or TNF-α to the OmpA/OprF chimeric sensor into a measurable output signal. An initial reporter was constructed using the CpxA-CpxR two component regulatory system which had previously been shown to be induced by the interaction of OmpA with a surface during biofilm formation (Ma and Wood, 2009). However, the reporter constructs, in which the *cpxR* or *cpxP* promoter drove the expression of GFP or β-galactosidase, were incapable of producing a measurable response to IFN-γ or TNF-α binding. Therefore, another regulatory system responsive to extracellular stress was required. The phage shock protein (*psp*) operon was selected, specifically the *pspA* promoter was used to drive *lacZ* expression as the reporter construct. The whole cell bioreporter expressing the OmpA/OprF sensor construct and the *pspA-lacZ* fusion reporter had a detection threshold of 300 pM for IFN-γ and 150 pM for TNF-α, upon addition of cytokines directly to bacterial culture. This was the first time that binding of a ligand to OmpA was shown to produce a measurable response by the *pspA* promoter.

The number of bacteria based sensors of which extracellular ligands bind to an outer membrane protein and elicit a response are limited, the bioreporter developed here expands the toolbox of synthetic biology to develop new extracellular sensors for compounds which do not enter the cell. Furthermore, the modularity of the extracellular loops of OmpA permit the development of multiple novel sensors systems using the bioreporter developed here. Nevertheless, there are areas where this novel system has room for improvement, such as the amplitude of the response needs be increased to reduce noise within the system. This could be achieved by teasing out the mechanism of signal transduction from OmpA to the inner membrane reporter

PspA and insulating this system from crosstalk with other systems. We hypothesis that the binding signal is transduced by means of the C-terminal of OmpA which interacts with the peptidoglycan layer, anchoring the outer membrane to the cell wall of *E.coli*. Moreover, the C-terminal of OmpA interacts with the Tol-Pal system, which is involved in maintaining outer membrane integrity, phage infection-and links the outer membrane to the inner membrane (Cascales et al., 2002). Specifically, OmpA interacts with the peptidoglycan associated lipoprotein, Pal of the TolB-Pal complex. The TolB-Pal complex is linked to the inner membrane associated proteins (TolQRA) by the C-terminal domain of TolA. TolA is energized by the proton motive force (PMF), such that changes in the PMF result in conformational changes of TolA altering the interaction of the inner and outer membrane associated Tol complexes. Conformational changes of TolA, potentially could alter energy transduction across the inner membrane by modifying the TolQ, TolR ion conducting channel (Vankemmelbeke et al., 2009). Changes in the proton motive force induce transcription of the *pspA* promoter, suggesting how ligand binding to OmpA produces a *pspA* response.

The third portion of the first goal was to determine the threshold detection limit for IFN-γ and TNF-α of the whole cell bioreporter in an *in vitro* model of a dysfunctional intestinal barrier. To simulate a dysfunctional barrier, the basolateral surface of Caco-2 cell monolayers were exposed to IFN-γ or TNF-α independently and in combination, reducing the TEER by 20% for individual cytokines and 30% in combination. The reduction in TEER permitted the paracellular transport of IFN-γ and TNF-α across the monolayer in a concentration dependent manner. Whole cell

bioreporters were applied directly to the apical chamber or "lumen" supernatant, application of pTCA4 improved detection by an order of magnitude (300 pM to 14 pM) compared to the addition of the supernatant to a bioreporter culture. Further, the detection threshold for pTCA6 improved by an order of magnitude for both IFN-γ (300 pM to 15.3 pM) and TNF-α (150 pM to 15.1 pM). The increase in sensitivity of the whole cell bioreporter may be the result of proximity of the bioreporter to the apical surface of the Caco-2 barrier. In initial assays, cytokines were applied directly to the bacterial culture such that the cytokines would have been equally distributed due to constant agitation of the culture. However, a gradient would form in the apical chamber such that the highest concentration of IFN-γ or TNF-α would be observed at the interface, due to a lack of agitation. Moreover, the lack of agitation may result in the settling of the bioreporter on the apical surface of the Caco-2 monolayer resulting in the interaction of the bioreporter with higher concentrations of the cytokines.

The finding that direct application of the bioreporter to the *in vitro* model of a dysfunctional barrier, increased the sensitivity of the bioreporter for IFN-γ and TNF-α, furthers the potential development of an orally administrated detection system for the inflammatory cytokines at the site of intestinal inflammation. Nevertheless, there are limitations to this method of testing as it does not account for flow rates which would be observed by the whole cell bioreporter in the intestinal tract and only a portion of the bioreporter would reach the site of inflammation, being exposed to the highest concentrations of IFN-γ or TNF-α. Further it does not account for the complex environment and plethora of environmental cues the bioreporter would be exposed to.

The whole cell bioreporter developed in the first objective was capable of detecting TNF-α at concentrations observed in the stool of IBD patients (15.8-343.8 pM), however, there is not an established IFN-γ concentration observed in the stool of IBD patients. Nevertheless, this whole cell biosensor could be used to detect Shigellosis at the site of attack, Small Intestinal Bacterial Overgrowth, or diseases of chronic inflammation such as cardiovascular disease or cystic fibrosis. Lastly, the cytokine detection system is not limited to detection of inflammation in the gut and could be used to detect IFN-γ or TNF-α present in urine, where a urinary tract infection may be present or IFN-γ in the sputum of Cystic Fibrosis patients. This study provides a new platform for the development of multiple extracellular sensors and a means to detect the inflammatory markers IFN-γ or TNF-α that pertain to multiple diseases.

As stated above, the second goal of this dissertation was to engineer a whole cell bioreporter system for the detection of approximated hyperuricemic concentrations of uric acid observed in the intestinal lumen. To this end, a detection system for uric acid harnessing the purine catabolism pathway of *B. subtilis* was engineered. The transcriptional regulator, *pucR,* was constitutively expressed in order to regulate the expression of a synthetic promoter in the presence of uric acid. A synthetic promoter was designed, to control the expression of GFP in which the spacer region (between the -10 and -35 consensus sequences) of the chloramphenicol promoter was replaced with the *pucR* box. The original hypothesis was that PucR bound uric acid would down regulate the production of GFP by binding to the *pucR* box of the synthetic promoter, hindering expression of GFP. However, the opposite was observed, such that GFP production was upregulated in the presence of uric acid

which may be explained by the strand orientation of the *pucR* box.

The reporter was capable of significantly differentiating between the calculated uric acid concentrations in the intestinal lumen at homeostasis (48.3 μM) and hyperuricemic concentrations (≥ 88.7 μM) and the minimal concentration of differentiation was 75 μM. The overall amplitude of the reporter needs to be increased in this system. This could be achieved by the addition of an enhancer site upstream of the promoter or modification of the spacer region size or optimization of the -10 and -35 sequences. The most interesting aspect of this system was that the pucR box of the synthetic promoter enhanced GFP production when expressed in *E. coli* (gram negative), however, in *B. subtilis* (gram positive) placement of the *pucR* box within the spacer region or overlapping the -10 or -35 consensus sequence resulted in negative regulation of the gene. This difference in promoter regulation seen between *E. coli* and *B. subtilis* with respect to a *pucR* controlled promoter has not been demonstrated before.

The two whole cell bioreporter systems developed in this dissertation expand the toolbox of available sensors that can be deployed for the detection of individual environmental factors. In particular, the capacity of OmpA loops to be replaced with various peptide fragments provides a platform for the development of new ligand binding proteins which induce a quantifiable signal is a substantial contribution to the development of bacteria based bioreporter system. The modularity of both systems permits them to be integrated into a single bacteria for the detection of multiple environmental cues simultaneously. The reporters of the systems could be integrated with AND, OR circuits for the detection of diseases such as cardiovascular disease of

which chronic inflammation, hypertension (resulting from elevated uric acid) are direct risk factors to the development and progression of the disease. Further, detection of inflammation markers would indicate a permeable intestinal barrier which has been suggested as a contributing factor to cardiovascular disease, arthritis, cystic fibrosis and many other diseases. Lastly, to make the bioreporter system easier to be deployed for monitoring of disease progression in a patients home, induction of the reporters could control production and secretion of a dye, such as indigo, which has previously been produced in bacteria (Bhushan et al., 2000), to notify the patient of an issue after a bowel movement or the use in other detection applications (urine or sputum).

References

Bhushan B, Samanta SK, Jain RK. 2000. Indigo production by naphthalene-degrading bacteria. *Lett. Appl. Microbiol.* **31**:5–9. http://dx.doi.org/10.1046/j.1472-765x.2000.00754.x.

Cascales E, Bernadac A, Gavioli M, Lazzaroni J-C, Lloubes R. 2002. Pal Lipoprotein of Escherichia coli Plays a Major Role in Outer Membrane Integrity. *J. Bacteriol.* **184**:754–759. http://www.ncbi.nlm.nih.gov/pmc/articles/PMC139529/.

Limaye SA, Haddad RI, Cilli F, Sonis ST, Colevas AD, Brennan MT, Hu KS, Murphy BA. 2013. Phase 1b, multicenter, single blinded, placebo-controlled, sequential dose escalation study to assess the safety and tolerability of topically applied AG013 in subjects with locally advanced head and neck cancer receiving induction chemotherapy. *Cancer* **119**:4268–4276. http://dx.doi.org/10.1002/cncr.28365.

Ma Q, Wood TK. 2009. OmpA influences Escherichia coli biofilm formation by repressing cellulose production through the CpxRA two-component system. *Environ. Microbiol.* **11**:2735–2746. http://dx.doi.org/10.1111/j.1462-2920.2009.02000.x.

Mendis. S, Armstrong T, Bettcher D, Branca F, Lauer J, Mace C, Poznyak V, Riley L, Silva VDCE, Stevens G. 2014. Global Status Report on Noncommunicable Disease 2014. *World Heal. Organ.* http://apps.who.int/iris/bitstream/10665/148114/1/9789241564854_eng.pdf?ua=1

Vankemmelbeke M, Zhang Y, Moore GR, Kleanthous C, Penfold CN, James R. 2009. Energy-dependent Immunity Protein Release during tol-dependent Nuclease

Colicin Translocation. *J. Biol. Chem.* **284**:18932–18941.

http://www.ncbi.nlm.nih.gov/pmc/articles/PMC2707214/.

APPENDIX ONE

Supplemental Figures

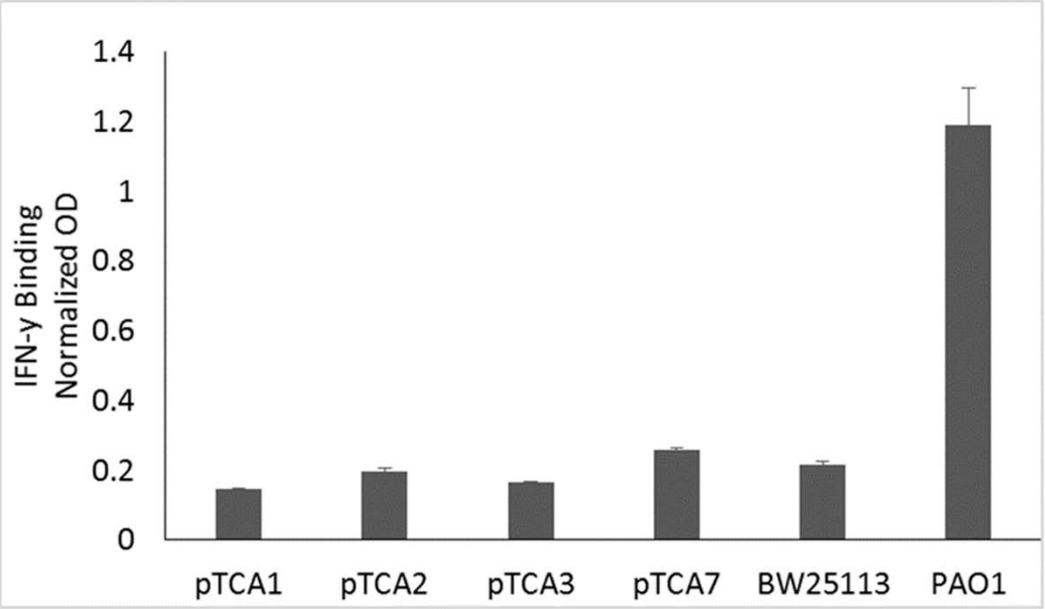

Figure S2.1: Whole cell ELISA for detection of bound IFN-γ. Fixed cells were standardized to an OD_{600} of 0.5 in PBS and incubated with 1μg/mL of IFN-γ overnight. Bound IFN-γ was determined using biotin labeled anti-human IFN-γ antibody at a 1:500 dilution, and detected with streptavidin labeled HRP. Absorbance was measured 450nm and 550nm, the mean of three independent experiments (five samples) is represented, error bar represent 95% confidence intervals.

APPENDIX TWO

Supplemental Tables

Table S2.1: Primers used in this study

Table S1: Primers used in this study

Name	Sequence 5' to 3'
pSC101_F	CTGCAGGAAAGCATGCAAAGGTACC
pSC101_R	GCGGCCGCTTTACATGTTTTGAATTC
pBAC-LacZ_F	ATGACCATGATTACGAATTTCGACC
pBAC-LacZ_R	CATGAGCGGATACATATTTGAATGTATTTAG
OmpA_F	AATTCAAAACATGTAAAGCGGCCGCATATGCCTGACGGAGTTC
OmpA_R	TGCATGCTTTCCTGCAGTTAAGCCTGCGGCTGAGT
OmpAL1_F	GCGCTGGTGCTTTTGGTGGTTACC
OmpAL1_R	TCATGGTACTGGGACCAGCCCAG
OmpAL2_F	CTCAGGGCGTTCAACTGACCGCTAA
OmpAL2_R	AGTCGTAACCCATTTCAAAGCCAACATACG
OmpAL3_F	ACACCGGCGTTTCTCCGGTC
OmpAL3_R	GAGTGTAGATGTCCAGGTCGTCAGTGATTG
OAL1_FL1_F	GTCCCAGTACCATGACGCAACATGAAGAACGCGGACGCGCTGGTGCTTTTG
OAL1_FL1_R	CAAAAGCACCAGCGCGTCCGCGTTCTTCATGTTGCGTCATGGTACTGGGAC
OAL2_FL2_F	GAAATGGGTTACGACTGGCACCTACGAAACCGGCAACAAGAAGGTCCACTACAAAGCTCAGGGC
OAL2_FL2_R	GCCCTGAGCTTTGTAGTGGACCTTCTTGTTGCCGGTTTCGTAGGTGCCAGTCGTAACCCATTTC
OAL3_FL3_F	GGACATCTACACTCAACATCAACAGCGACAGCCAAGGCCGTCAGACACCGGCGTTTCTC
OAL3_FL3_R	GAGAAACGCCGGTGTCTGACGGCCTTGGCTGTCGCTGTTGATGTTGAGTGTAGATGTCC
OAL1_FL5_F	GTCCCAGTACCATGAGACGTTTGCTCCGACTCCGACAACGACG
OAL1_FL5_R	CAAAAGCACCAGCGCGCGTACGACTTCGGCGACAG
OAL1_FGL5*_F	**CCGAAAGATAACACCTGGTACACTGGTGCTAAACTGGGCTGGTCCTGCTCCGACTCCGAC**
OAL1_FGL5*_R	**GGGTTAACCTGGTAACCACCAAAAGCACCAGCGCCCAGTTGATCCGGGCACTTGTCGACG**
OAL2_FL6_F	GAAATGGGTTACGACTGCTGACATCAAGAACCTGGCTGACTTCATG
OAL2_FL6_R	GAGCTTTGTAGTGGACCGGTGGTGGAAGTGGACGG
OAL2_FGL6*_F	**GTGGTTACCAGGTTAACCCGTATGTTGGCTTTGAAATGGGTTACGACTGGGACGTGAAGTTCGACTTCGA**
OAL2_FGL6*_R	**GTCAGTGATTGGGTAACCCAGTTTAGCGGTCAGTTGAACGCCCTGGTTCTTGATGTCAGCGTAGCTGT**
OAL3_FL7_F	CTGGACATCTACACTCGGTGGTCGCGTGAACACACCGGCGTTTCTC
OAL3_FL7_R	GAGAAACGCCGGTGTGTTCACGCGACCACCGAGTGTAGATGTCCAG
PspApro_F	TATGTATCCGCTCATGTGCGAGATGCGAAACCTG
PspApro_R	CGTAATCATGGTCATAATGTTGTCCTCTTGATTTCTGCGTTC

* denote primers based on Gilleland model (18)

FL denotes the donor loop insert of OprF based on Rawling model (16)